Journal of Medicinal Chemistry

ARTICLE

pubs.acs.org/jmc

Discovery of a Series of Imidazo[4,5-*b*]pyridines with Dual Activity at Angiotensin II Type 1 Receptor and Peroxisome Proliferator-Activated Receptor-γ

Agustin Casimiro-Garcia,* Gary F. Filzen,* Declan Flynn, Christopher F. Bigge, Jing Chen, Jo Ann Davis, Danette A. Dudley, Jeremy J. Edmunds, Nadia Esmaeil, Andrew Geyer, Ronald J. Heemstra, Mehran Jalaie, Jeffrey F. Ohren, Robert Ostroski, Teresa Ellis, Robert P. Schaum, and Chad Stoner

Pfizer Global Research and Development, Groton Laboratories, Eastern Point Rd, Groton, Connecticut 06340, United States

Supporting Information

ABSTRACT: Mining of an in-house collection of angiotensin II type 1 receptor antagonists to identify compounds with activity at the peroxisome proliferator-activated receptor-γ (PPARγ) revealed a new series of imidazo[4,5-*b*]pyridines **2** possessing activity at these two receptors. Early availability of the crystal structure of the lead compound **2a** bound to the ligand binding domain of human PPARγ confirmed the mode of interaction of this scaffold to the nuclear receptor and assisted in the optimization of PPARγ activity. Among the new compounds, (*S*)-3-(5-(2-(1*H*-tetrazol-5-yl)phenyl)-2,3-dihydro-1*H*-inden-1-yl)-2-ethyl-5-isobutyl-7-methyl-3*H*-imidazo[4,5-*b*]pyridine (**2l**) was identified as a potent angiotensin II type I receptor blocker (IC_{50} = 1.6 nM) with partial PPARγ agonism (EC_{50} = 212 nM, 31% max) and oral bioavailability in rat. The dual pharmacology of **2l** was demonstrated in animal models of hypertension (SHR) and insulin resistance (ZDF rat). In the SHR, **2l** was highly efficacious in lowering blood pressure, while robust lowering of glucose and triglycerides was observed in the male ZDF rat.

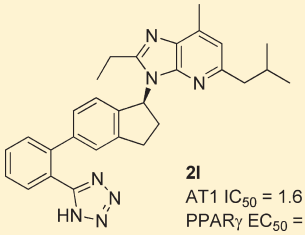

2l
AT1 IC_{50} = 1.6 nM
PPARγ EC_{50} = 212 nM (31%max)

INTRODUCTION

Hypertension and insulin resistance are intimately linked and constitute two components of the metabolic syndrome or Syndrome X. Patients with metabolic syndrome are characterized as having three or more of the following comorbidities: impaired fasting glucose, hypertriglyceridemia, hypertension, low high-density lipoprotein cholesterol levels, and central obesity.[1] Hypertension is a condition with a well understood pathophysiology with a number of pharmaceuticals such as diuretics,[2] beta blockers,[3] angiotensin converting enzyme inhibitors (ACE inhibitors),[4] calcium channel antagonists,[5] angiotensin receptor blockers[6] (ARBs), and more recently renin inhibitors[7] being prescribed for safe and effective treatment. It has been found that 29% of U.S. adults >18 years of age are hypertensive with equal prevalence among men and women.[8] Approximately 90 million patients exhibit insulin resistance (prediabetes), and 44 million are both hypertensive and insulin resistant.

The development of insulin resistance is a critical step in the evolution of type 2 diabetes, and the increasing prevalence of central obesity has contributed significantly to this situation. Patients with diabetes mellitus are at increased risk for premature disability and death associated with vascular complications. Additionally, individuals with prediabetes (impaired glucose tolerance and/or impaired fasting glucose with concomitant hyperinsulinemia) suffer atherosclerotic vascular events more frequently than in the general population.[9] Evidence suggests that there is a continuous relationship between blood glucose level and macrovascular disease with no obvious threshold. Indeed, a recent study showed a clear relationship between HbA1c and cardiovascular (CV) risk even within a nondiabetic range.[10] Insulin resistance can be treated through diet modification and exercise[11] and also through pharmaceutical intervention using, in combination or as standalone therapy, biguanides, sulfonylureas, glucagon-like peptide-1 (GLP-1) analogues,[12] dipeptidyl peptidase 4 (DPP-4) inhibitors,[13] and the thiazolidinedione (TZD) class of drugs. TZDs function through insulin sensitization by activation of the nuclear hormone receptor peroxisome proliferator activated receptor-γ (PPARγ), though recent evidence suggest that these drugs may in fact function by blocking a phosphorylation cascade.[14] A consequence of simultaneously treating several comorbidities is that a significant pill burden is placed on the patient, often leading to issues with compliance and unforeseen drug−drug interactions. Currently, there are no therapies whereby both hypertension and insulin resistance can be simultaneously treated with the same pharmaceutical agent. ARBs are a highly regarded class of drugs used for the treatment of hypertension.[15] They are safe and effective with few side effects. One particular ARB, telmisartan (Figure 1), a potent selective AT1 receptor antagonist, was reported to also have weak activity at PPARγ.[16] Telmisartan's pharmacokinetic

Received: April 6, 2011
Published: May 10, 2011

Scheme 1. Synthesis of New Imidazo[4,5-*b*]pyridine Derivatives 2[a]

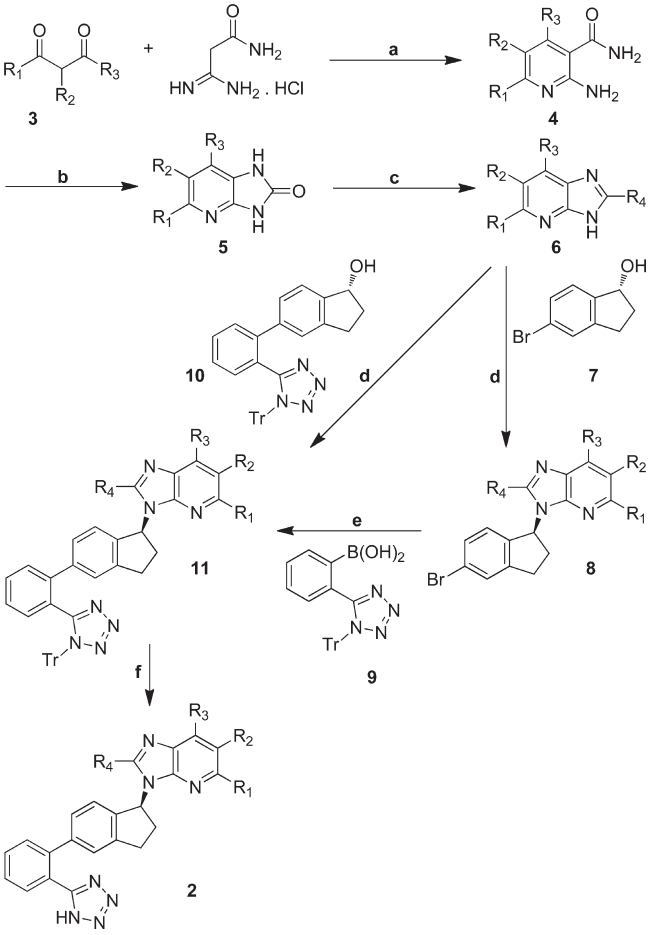

[a] Reagents and conditions: (a) KOH, MeOH; (b) $PhI(OAc)_2$, KOH, MeOH, 0 to 25 °C; (c) $MgCl_2$, $(R_4CO)_2O$, R_4CO_2H, 120 °C, 24 h; (d) **7** or **10**, DEAD, Ph_3P, THF, 0 to 25 °C; (e) **9**, $Pd(OAc)_2$, Ph_3P, K_2CO_3, DME-H_2O, 80 °C, 18 h; (f) 3 M HCl, acetone.

(PK) profile confers 24 h blood pressure (BP) lowering and reduced BP variability compared to other ARBs. Additionally, small clinical trials have demonstrated that telmisartan is capable of improving glycemic parameters in metabolic syndrome patients[17] compared to another ARB (losartan) suggesting the effect is not an AT1 receptor mediated phenomenon. The improvements seen in the glycemic parameters of metabolic syndrome patients taking telmisartan versus patients taking other ARBs could be reasonably attributed to telmisartan's weak activity at PPARγ. Efforts to identify the structural features responsible for the PPARγ activity of telmisartan have been reported.[18−20] In addition, telmisartan analogues have been designed and reported as dual PPARγ agonist/AT1 antagonists.[21−23] During the course of our research, a novel chemical scaffold **2** (Figure 1) was discovered which allowed for interaction with both PPARγ and angiotensin II type 1 (AT1) receptor.[24] A pharmaceutical agent with the dual activity of AT1 inhibition and partial PPARγ agonism could potentially treat several recognized CV risk factors including hypertension, insulin resistance, and hypertriglyceridemia in patients with metabolic syndrome.

The novel scaffold **2** was identified by mining our proprietary collection of compounds and data from previous PPARγ and ARB programs. Our strategy involved cross screening of known PPARγ agonists for ARB activity using an AT1 competition radioligand binding assay, as well as screening of known ARBs for PPARγ activity in a human PPARγ chimeric receptor transactivation assay. The same treatment was given to marketed ARBs (losartan, candesartan, valsartan) and marketed PPARγ agonists (pioglitazone and rosiglitazone). Our screening efforts led to the unique indanyl-based scaffold **2** derived from a previous ARB program[25,26] that showed robust AT1 activity and partial activation of PPARγ. In this report, optimization of the novel scaffold and identification of **2l**, a potent AT1 antagonist with partial PPARγ activity with demonstrated efficacy in animal models of hypertension and insulin sensitization, are described.

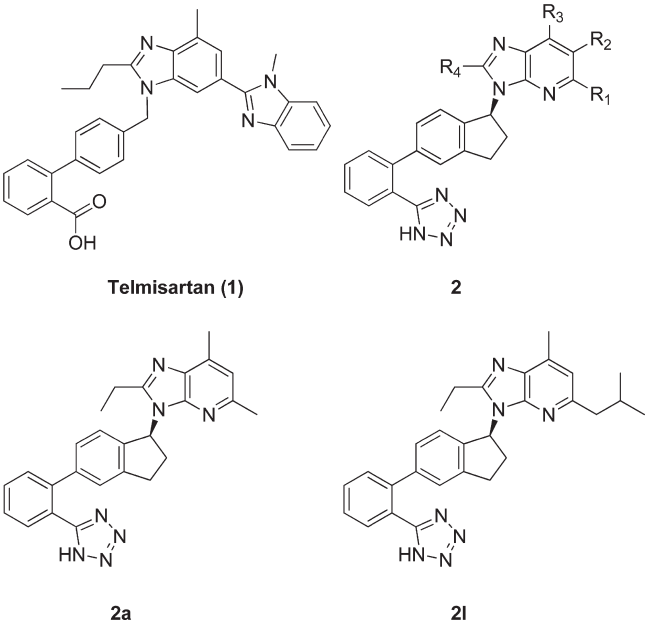

Figure 1. Chemical structures of telmisartan (**1**), new scaffold **2**, and imidazopyridines **2a** and **2l**.

CHEMISTRY

The synthesis of the new imidazo[4,5-*b*]pyridine derivatives **2** is shown in Scheme 1. The imidazo[4,5-*b*]pyridine headgroup **6** was prepared in three steps from an appropriately substituted 1,3-diketone **3** according to a procedure described by Senanayake and collaborators.[27] Condensation of diketone **3** with amidinoacetamide hydrochloride in the presence of potassium hydroxide and methanol provided amide **4**. In the case of unsymmetrical 1,3-diketones, this condensation led to a mixture of regioisomers favoring the product containing the largest R group at C-6. This mixture was not separated but taken directly into the next step. Hoffmann rearrangement of amide **4** afforded imidazolone **5**, which was then converted into the corresponding imidazo[4,5-*b*]pyridines **6** by reaction with a mixture of an organic acid and anhydride containing the desired R_4 group. The (*R*)-5-bromo-1-indanol (**7**) was prepared via catalytic enantioselective reduction of 5-bromo-1-indanone using (*S*)-methyl-CBS-oxazaborolidine and borane-dimethyl sulfide complex.[28,29] For the determination of enantiomeric purity, racemic **7** was prepared by sodium borohydride reduction of 5-bromo-1-indanone. Indanol **7** was obtained with >99% ee as determined by chiral chromatography. Mitsunobu reaction of

dx.doi.org/10.1021/jm200409s |*J. Med. Chem.* 2011, 54, 4219–4233

Scheme 2. Synthesis of Carboxylic Acid 14[a]

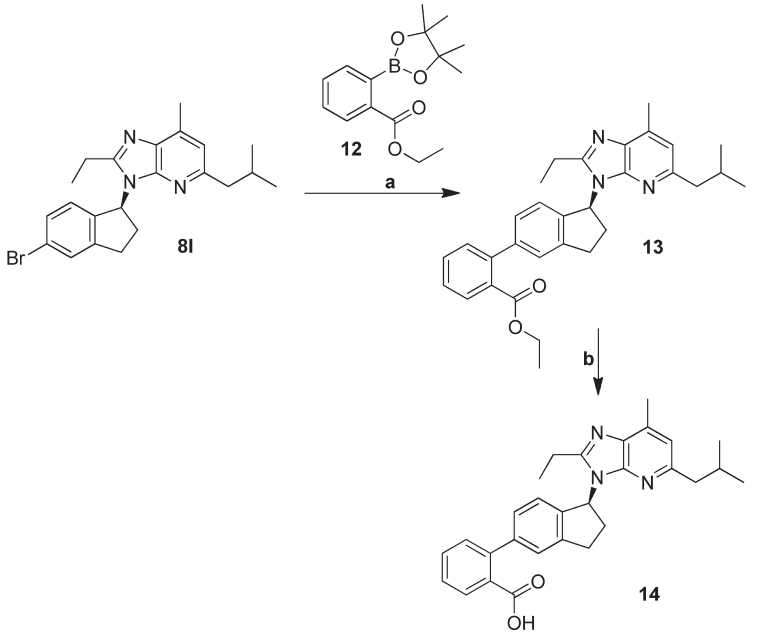

[a] Reagents and conditions: (a) **12**, $PdCl_2(dppf)$, Na_2CO_3, dioxane-H_2O, 85 °C, 18 h; (b) 1 M NaOH, 100 °C, 24 h.

imidazopyridine **6** with bromo-indanol **7** using diethylazodicarboxylate and triphenylphosphine in THF provided **8**. Suzuki cross-coupling of bromide **8** with boronic acid **9**[30] in the presence of catalytic palladium acetate, triphenylphosphine, and potassium carbonate in DME-water gave **11**. Alternatively, trityl-protected tetrazole **11** was obtained in a single step from imidazopyridine **6** using the more elaborated indanol **10**. This intermediate was prepared from bromide **7** and boronic acid **9** using the Suzuki cross-coupling conditions mentioned earlier. Mitsunobu reaction of imidazopyridine **6** with indanol **10** was accomplished under similar conditions as those described above to provide **11**. To complete the synthesis of the desired compounds, removal of the trityl group under the conditions of 3 M HCl in acetone afforded the desired tetrazole derivatives **2**. Assesment of enantiomeric purity of **2l** was accomplished by (i) synthesis of racemic **2l** following the same sequence described in Scheme 1, but departing from racemic **7**; (ii) determination of enantiomeric purity using chiral chromatography with a chiralpak AD-H column and SFC conditions, and using racemic **2l** for the analysis. The enantiomeric purity of **2l** was determined to be 96.5% ee.

The synthesis of carboxylic acid analogue **14** is depicted in Scheme 2. Suzuki cross-coupling of bromide **8l** and boronate ester **12** under the conditions described previously afforded ester **13**. Ester hydrolysis of **13** using sodium hydroxide in methanol–water afforded **14**.

Preparation of **2a**–**c**, **2e**, and **15** has been previously described.[25,26,31]

RESULTS AND DISCUSSION

As mentioned earlier, affinity for the AT1 receptor was determined utilizing human recombinant AT1 receptors in a competition radioligand binding assay with [^{125}I]Tyr^4-Sar^1,Ile^8-Angiotensin II. The IC_{50} values of the imidazo[4,5-*b*]pyridine derivatives are displayed in Table 1. Activation of human PPARγ was determined using a chimeric receptor (PPARγ ligand binding domain (LBD)/ Gal4 DNA binding domain) transactivation assay. The EC_{50} values and the percent of maximal activation with darglitazone[32] as a reference full agonist (defined as 100% effect) are presented in Table 1. Telmisartan and pioglitazone are included as reference compounds.

The novel scaffold **2** was identified from this cross-screening approach. Imidazopyridine **2a** (Figure 1) demonstrated potent AT1 antagonist activity and partial PPARγ agonism (AT1 IC_{50} = 7.6 nM; PPARγ EC_{50} = 591 nM, 24% activation). With this scaffold in hand, efforts were directed to improve PPARγ activity while improving or maintaining the inherent AT1 potency. The SAR associated with the AT1 binding activity of this class of compounds is well-understood;[26,31] however, we had limited information about how these compounds interacted with PPARγ. Past experience with nuclear hormone receptors[33,34] and initial docking studies suggested that these compounds might bind in a typical agonist conformation with the carboxylic acid headgroup or carboxylic acid bioisostere tetrazole forming a hydrogen bond network with the three charge clamp residues, Tyr327, His 449, and His323 (Figure 2).[35,36] The modeling studies also suggested that the central aryl core bound within the hydrophobic pocket formed by helices 3, 6, and 10 and the lipophilic tail was buried in the hydrophobic cleft in the anterior of the receptor. To our surprise, the 2.4 Å resolution crystal structure of **2a** complexed with the LBD of human PPARγ (Figure 3) revealed a completely flipped binding mode (see Supporting Information S-Table 1 for X-ray data collection and structure refinement statistics). The lipophilic tail is projected into the AF-2 domain pocket of the receptor and interacts with the charge clamp residues through nonpolar, van der Waals interactions. The crystal structure also revealed that the acidic tetrazole motif is buried in the hydrophobic anterior of the receptor and makes a weak H-bond interaction between the N-2 of the tetrazole ring and Arg288 (2.7 Å distance).

dx.doi.org/10.1021/jm200409s |*J. Med. Chem.* 2011, 54, 4219–4233

Table 1. AT1 and PPARγ Transactivation Activity of Imidazo[4,5-*b*]pyridine Derivatives 2a−o, 14, and 15

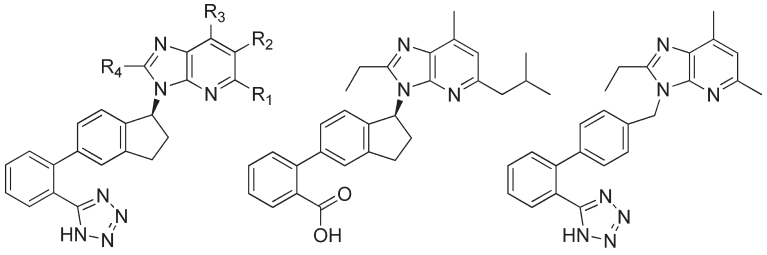

2 **14** **15**

compound	R_1	R_2	R_3	R_4	AT1 IC_{50} (nM)	h-PPARγ EC_{50} (nM)[a] (% max)[b]
Telmisartan					0.49	1520 (33)
Pioglitazone					-	1280 (80)
2a (*S*)[c]	Me	H	Me	Et	7.6	591 (24)
2b (rac)	Me	H	Me	Et	96	574 (16)
2c (*R*)[c]	Me	H	Me	Et	661	2620 (20)
2d	Me	H	Me	n-propyl	13.3	1320 (24)
2e (rac)	Me	H	Me	n-butyl	238	2200 (28)
2f	Me	H	Me	i-propyl	10.2	295 (19)
2g	Me	H	Me	c-propyl	8.2	762 (24)
2h	Me	Me	Me	Et	202	1820 (23)
2i	Me	Et	Me	Et	15.7	1340 (25)
2j	Et	H	Me	Et	6.8	494 (26)
2k	Et	H	Me	i-propyl	16.9	264 (23)
2l	i-butyl	H	Me	Et	1.6	212 (31)
2m	i-butyl	H	Me	i-propyl	3.5	89 (25)
2n	Me	H	i-butyl	Et	748	165 (28)
2o	benzyl	H	Me	Et	5.2	90 (27)
14					10.5	175 (33)
15					2.7	>20000 (7)

[a] TA (transactivation assay). Mean value of at least two determinations. [b] The maximal efficacy of darglitazone in the PPARγ activation assay was defined as 100%. [c] Stereochemistry of the chiral center. Unless specified, all compounds were prepared as the (*S*)-enantiomer.

Interestingly, despite the lack of direct engagement with the charge clamp and the AF-2 activation motif this and other compounds in this series retain appreciable PPARγ agonist activity as discussed below.

Availability of the set of compounds **2a−c** in our compound collection provided an opportunity to examine the effect of the stereochemistry at C-1 of the indane ring on the AT1 and PPARγ activity. The (*S*)-enantiomer **2a** exhibited potent activity for both receptors (AT1 IC_{50} = 7.6 nM; PPARγ EC_{50} = 591 nM, 24% activation), while the (*R*)-enantiomer **2c** exhibited a significant drop in AT1 activity with only a moderate change in PPARγ potency (AT1 IC_{50} = 661 nM; PPARγ EC_{50} = 2620 nM, 20% activation). AT1 potency for racemic **2c** was reduced when compared to (*S*)-enantiomer **2a**, while it retained similar potency for PPARγ (AT1 IC_{50} = 96 nM; PPARγ EC_{50} = 574 nM, 16% activation). The effect of opening the indane ring was investigated with the known benzyl analogue **15**.[31] This compound was reported as a potent AT1 receptor antagonist and this was corroborated in our screen (IC_{50} = 2.7 nM). Interestingly, **15** was completely devoid of PPARγ activity (EC_{50} > 20 000 nM, 7% activation) demonstrating that conformational restriction derived from the indane ring is required for PPARγ activity. Guided by this data, synthetic efforts were focused on indane derivatives in the (*S*)-enantiomer series.

Analysis of the complex of **2a** bound to human PPARγ-LBD revealed areas that could be utilized to improve interaction with this receptor. Modification of R_4 (Figure 1) with both linear and branched alkyl groups appeared attractive to improve interaction with PPARγ, as there are several hydrophobic residues that surround this region of the molecule, as well as a large volume which could potentially accommodate larger substituents. Increasing the length of R_4 (Table 1) from ethyl in **2a** to either propyl in **2d** (AT1 IC_{50} = 13.3 nM; PPARγ EC_{50} = 1320 nM, 24% activation) or butyl in **2e** (AT1 IC_{50} = 238 nM; PPARγ EC_{50} = 2200 nM, 24% activation) led to loss of potency in both AT1 and PPARγ. It should be noted that **2e** was racemic and no efforts to obtain the (*S*)-enantiomer were pursued due to poor AT1 activity. Modification of R_4 to cyclopropyl in **2g** (AT1 IC_{50} = 8.2 nM; PPARγ EC_{50} = 762 nM, 24% activation) or isopropyl in **2f** (AT1 IC_{50} = 10.2 nM; PPARγ EC_{50} = 295 nM, 19% activation) was well tolerated. Data from this set of compounds showed that both ethyl and isopropyl are suitable R_4 substituents in order to obtain potent dual AT1 and PPARγ activity.

The effect of modifying the R_2 group on the AT1 activity was uncertain as this position was not previously modified. On the basis of the complex of **2a** bound to human PPARγ-LBD, it appeared to be a less attractive location to improve interaction with PPARγ. As such, only a limited set of analogues were prepared with

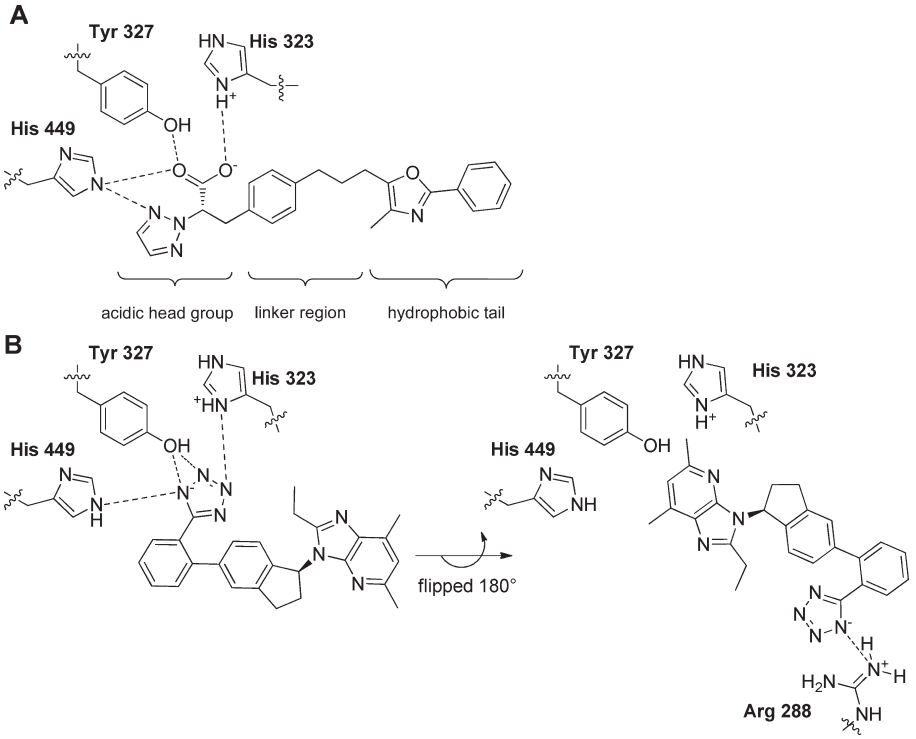

Figure 2. (A) Simplified ligand topology and simplified binding interaction map for a typical PPARγ full-agonist.[34,37] (B) Initial docking poses of **2a** bound in an agonist conformation to the PPARγ LBD suggested that the tetrazole moiety might interact with the charge clamp residues His323, His449, and Tyr327. This binding mode was subsequently shown by X-ray crystallography to be flipped 180° in the horizontal plane.

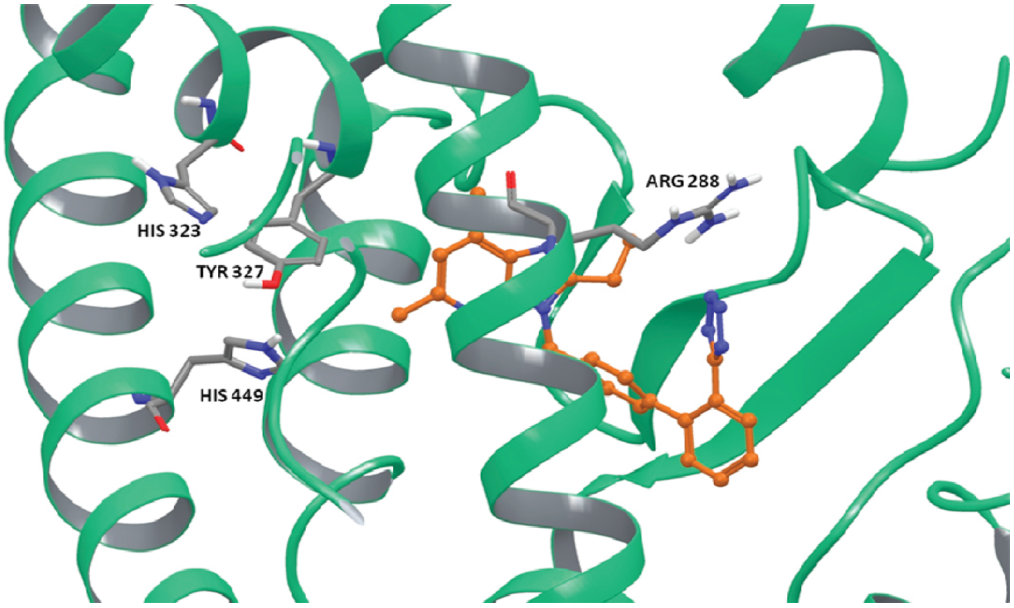

Figure 3. Three-dimensional representation of **2a** (gold) bound in the ligand binding pocket of human PPARγ (green ribbons and β-sheets with gray residues). The AF-2 helix which is partially disordered due to the lack of direct interactions between the ligand and the charge clamp residues is shown on the left-hand side of the figure. The compound wraps around helix 3 that lies in the middle. Formation of an H-bond between N-2 of the tetrazole ring and Arg288 (2.7 Å distance) was observed as was multiple hydrophobic interactions within the pocket.

modifications at this position. Substitution with methyl in **2h** (AT1 IC_{50} = 202 nM; PPARγ EC_{50} = 1820 nM, 23% activation), or ethyl in **2i** (AT1 IC_{50} = 16 nM; PPARγ EC_{50} = 1340 nM, 25% activation) was detrimental for activity at both receptors and no further expansion at this position was performed.

On the basis of the complex of **2a** bound to human PPARγ-LBD, two areas that looked promising to improve interaction with PPARγ were substitutions at R_1 and R_3 on the imidazopyridine ring. The substitution of R_1 appeared optimal to increase interaction with PPARγ as both lipophilic and hydrophilic

dx.doi.org/10.1021/jm200409s |J. Med. Chem. 2011, 54, 4219–4233

pockets were identified that could be reached with appropriate R_1 substitution. With the above observations in hand, modifications of the R_1 group were evaluated. Increasing the size of R_1 with ethyl as seen in **2j** (AT1 IC_{50} = 6.8 nM; PPARγ EC_{50} = 494 nM, 26% activation) and **2k** (AT1 IC_{50} = 16.9 nM; PPARγ EC_{50} = 264 nM, 23% activation) was well tolerated. Further increasing the size of R_1 to isobutyl led to **2l** (AT1 IC_{50} = 1.6 nM; PPARγ EC_{50} = 212 nM, 31% activation), a compound with improved potency at both receptors that maintained partial PPARγ agonism. Combining isobutyl at R_1 and isopropyl at R_4 provided **2m** (AT1 IC_{50} = 3.5 nM; PPARγ EC_{50} = 89 nM, 31% activation), a potent analogue with markedly improved potency at PPARγ. To further examine the space surrounding the R_1 substituent, a larger benzyl group was incorporated in **2o** (AT1 IC_{50} = 5.2 nM; PPARγ EC_{50} = 90 nM, 27% activation) that also showed potent activity at both receptors. Not surprisingly, large hydrophobic substituents led to marked improvements in PPARγ activity as there are several lipophilic residues in this region. The data obtained with **2j**−**m** and **2o** suggested that potency for both receptors can be modulated through appropriate selection of the R_1 group. Modification of R_3 substituents was briefly examined with **2n** (AT1 IC_{50} = 748 nM; PPARγ EC_{50} = 165 nM, 28% activation) which incorporated an isobutyl at such position. Results with this compound suggested that there was a limited opportunity to modify R_3 without compromising AT1 activity.

Tetrazoles are common bioisosteres of carboxylic acids,[38] and both moieties have been used extensively in the field of AT1 antagonists.[39,40] The impact of replacing tetrazole with a benzoic acid moiety in the current series was assessed with **14** (AT1 IC_{50} = 10.5 nM; PPARγ EC_{50} = 175 nM, 33% activation) that incorporated isobutyl for R_1 and ethyl for R_4. The tetrazole to carboxylic acid change appeared to mainly affect AT1 activity as observed with the approximately 7-fold drop in potency when comparing AT1 IC_{50} values for **14** to **2l**.

Imidazopyridine **2l** was identified with potent AT1 binding affinity (K_i = 0.69 nM) and showed an IC_{50} value (IC_{50} = 1.6 nM) that was only 3-fold lower than telmisartan. Other compounds in this series exhibited >5-fold reduction in AT1 potency when compared to telmisartan as assessed by their IC_{50} values. Retaining AT1 potency similar to that of telmisartan was an important criterion for advancing compounds into further studies. Furthermore, imidazopyridine **2l** exhibited improved PPARγ potency (PPARγ EC_{50} = 212 nM, 31% activation) when compared to that of telmisartan and retained partial agonism. On the basis of this potency, **2l** was selected for additional profiling. Imidazopyridine **2l** exhibited a high degree of selectivity over AT2 (K_i >10 000 nM). The AT1 receptor antagonist class can be divided into surmountable and insurmountable antagonists based upon their functional effects in assays such as isolated rabbit aorta.[41,42] Examples include losartan,[42] which is a classic competitive antagonist (surmountable) and telmisartan, which is an insurmountable antagonist,[43] wherein the observed pseudoirreversible blockade is driven by a very slow off rate from the AT1 receptor. It is believed that the very slow dissociation rate from the AT1 receptor contributes to the enhanced efficacy seen with this cohort of compounds. In order to characterize **2l** as a surmountable or insurmountable antagonist, a 96-well plate based method was developed. **2l** was incubated with the receptor at 10 μM to achieve complete receptor occupancy at equilibrium. Following washout of unbound compound, the receptor-compound complex was coincubated with the [^{125}I] radioligand at 3 × K_d to measure displacement of compound over time. As shown in Figure 4, imidazopyridine **2l** did not demonstrate any significant dissociation from the receptor over the time course of the assay. This profile was similar to that of telmisartan and strongly suggested an insurmountable profile.

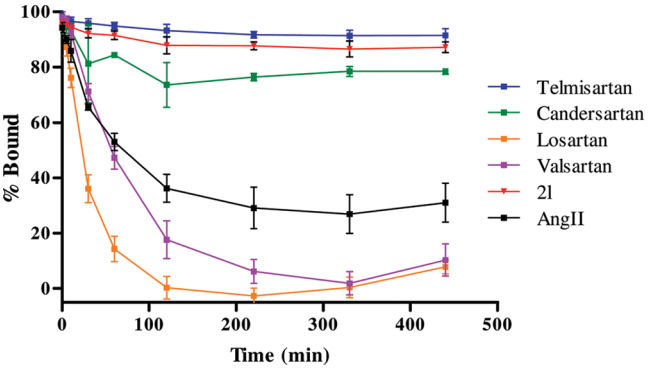

Figure 4. Dissociation of **2l** and reference ARBs from the AT1 receptor in a 96-well plate based assay (n = 3).

Table 2. Pharmacokinetic Properties of 2l in Rat

route	dose (mg/kg)	AUC (ng·h/mL)	$t_{1/2}$ (h)	F (%)	Cl (mL/min/kg)	V_{ss} (L/kg)
IV	1	1220	2.1		14	2.9
PO	5	4950		80		

Imidazopyridine **2l** was also screened in human PPARα and PPARβ chimeric receptor transactivation assays, and no detectable activity could be observed, thus demonstrating selectivity over these receptors. As the next step in this investigation was to perform studies in animal models of hypertension and diabetes, the pharmacokinetic properties of **2l** were evaluated in rat (Table 2) to determine if this compound would be suitable for oral administration. Bioavailability was high (80%) following a single 5 mg/kg dose. In vivo clearance and volume of distribution were moderate (Cl = 14 mL/min/kg; V_{ss} =2.9 L/kg). The measured half-life value was 2.1 h. The profile of **2l** was considered appropriate to progress into in vivo studies.

The dual pharmacology exhibited by **2l** required the use of two in vivo models to adequately assess this compound and define efficacy. First, **2l** was evaluated in the spontaneously hypertensive rat (SHR), a model that has been shown over decades to predict human antihypertensive efficacy. **2l** was administered orally to SHRs in a dose range from 0.3 to 10 mg/kg (n = 8 animals/group). After a single oral dose, **2l** demonstrated a dose-dependent sustained lowering of mean arterial BP with a maximal drop of 36 mmHg at 10 mg/kg (Figure 5). This was associated with a modest reflex tachycardia at the highest dose (+37 beats/min at 4−8 h post dose). Determination of systemic drug exposure for **2l** showed C_{max} and AUC of 74/283/3073 ng/mL and 320/1285/6833 ng·hr/mL, respectively, for the 1, 3, and 10 mg/kg doses. Telmisartan showed a similar dose−response profile (data not shown). Interestingly, BP remained suppressed for >20 h after a single dose of **2l**, and this was despite plasma levels of **2l** being undetectable at 20 h post dose. Upon cessation of dosing with **2l**, BP returned to predose levels in all animals. The magnitude of BP lowering seen with **2l** after single dose was consistent with historical in-house data for compounds in this

structural class. Further studies showed improved efficacy upon repeat dosing with once-a-day dosing for 7 days producing reductions in BP of >60 mmHg at 10 mg/kg. This was not due to compound accumulation but is consistent with the mechanism requiring 3−5 days to achieve maximal effects in rodents.

Imidazopyridine **2l** was also evaluated in the male Zucker diabetic fatty rat (ZDF), a model widely used to demonstrate insulin sensitization. Animals were placed on study at 6 weeks of age when they were insulin resistant but not yet diabetic as evident by euglycemia with concomitant plasma hyperinsulinemia. Control rats, when left untreated, will develop marked hyperglycemia, elevated triglycerides, and eventually loss of beta cell function and insulin insufficiency as the disease progresses. Compound **2l** was administered orally across a dose range of 0.1−100 mg/kg/day (n = 8 animals/group) for 40 days with pioglitazone (3 mg/kg) and telmisartan (100 mg/kg) included in the study as comparators. Insulin, glucose, triglycerides (TG), free fatty acids (FFA), adiponectin, HDL and VDL cholesterol, and body weight (BW) were monitored in this study. The effect of **2l** on the development of hyperglycemia in the ZDF rat is shown in Figure 6. Systemic exposure of **2l** in this strain of rat was determined in satellite animals dosed at 3, 10, and 100 mg/kg p.o. C_{max} values of 267/2730/176667 ng/mL and AUC of 4395/27973/2599853 ng·hr/mL, respectively, were calculated.

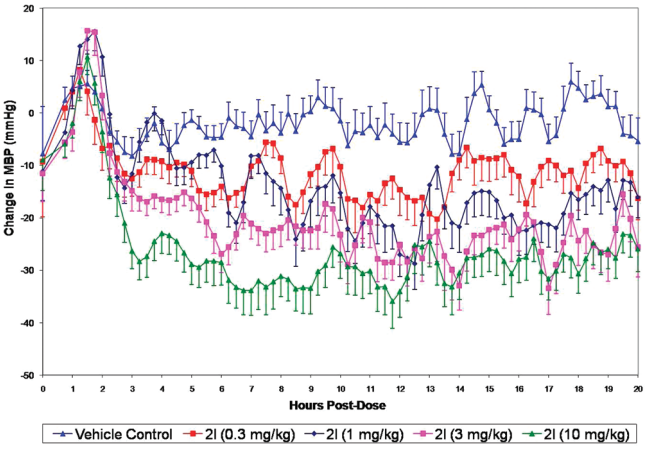

Figure 5. Effect of **2l** (0.3−10 mg/kg p.o.) on mean blood pressure in the SHR. All data represented as mean ± SEM, n = 8 animals/group.

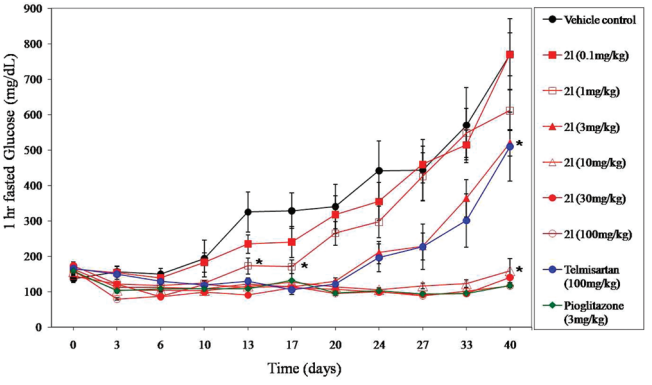

Figure 6. Effect of **2l** (0.1−100 mg/kg p.o. once daily for 40 days) on blood glucose in the male ZDF rat. All data represented as mean ± SEM, n = 8 animals/group. * p < 0.05 vs vehicle control.

The results show a time dependent increase in hyperglycemia in the vehicle treated rats with concomitant increases in TG, FFA and reduction in adiponectin (Table 3). Compound **2l** prevented the changes in a dose dependent fashion with the lower doses delaying the progression to overt diabetes and the higher doses preventing it altogether. At doses of 10 mg/kg and higher, **2l** maintained euglycemia, kept TG at baseline values, and doubled adiponectin levels relative to control by the end of the study. The improvement in metabolic phenotype was marked and at least equivalent to that of pioglitazone 3 mg/kg in this study. Interestingly, this efficacy was associated with a lower degree of bodyweight gain than was seen in the TZD group (Table 3 and Figure 7). Compared to vehicle controls, body weight gain was much greater for the pioglitazone group with significant (p < 0.05) increases in weight gain seen as early as day 6. The growth curves continued to diverge throughout the study with total weight gain in these animals being double that seen in vehicle controls. Telmisartan (100 mg/kg) induced modest increases of weight that achieved statistical significance from control at day 32. Since there are no reports of weight gain associated with the clinical use of telmisartan,[44] this is more likely a reflection of a "failure to thrive" in the control animals rather than a PPARγ effect of telmisartan. Certainly, the weight gain seen in control animals starts to plateau at day 28 (10 weeks old) and might reflect significant loss of calories through glycosuria. Compound **2l** showed increases in weight gain, which were statistically significant at 3 mg/kg with this dose causing gains similar to telmisartan. Doses of 10−100 mg/kg produced a greater degree of weight gain although this was not dose dependent and

Table 3. Evaluation of 2l in Male ZDF Rats[a]

treatment	dose (mg/kg/day)	glucose (mg/dL)	triglycerides (mg/dL)	BW gain (g)[b]	adiponectin (μg/mL)
Vehicle		771 ± 60[d]	618 ± 52	133 ± 9	11.9 ± 1.5
Pioglitazone	3	118 ± 4[c]	316 ± 29[c]	269 ± 4[c]	30.5 ± 1.2[c]
Telmisartan	100	510 ± 97[c]	935 ± 76	157 ± 4[c]	13.2 ± 1.5
2l	0.1	771 ± 100	559 ± 62	128 ± 10	9.9 ± 1.0
	1	612 ± 57	725 ± 69	150 ± 7	10.2 ± 0.9
	3	520 ± 37[c]	734 ± 73	159 ± 7[c]	11.4 ± 1.5
	10	159 ± 34[c]	393 ± 41	200 ± 5[c]	24.4 ± 2.0[c]
	30	140 ± 25[c]	288 ± 43[c]	202 ± 6[c]	24.3 ± 1.8[c]
	100	116 ± 5[c]	151 ± 11[c]	202 ± 6[c]	27.5 ± 1.0[c]

[a] All data mean ± SEM, n = 8 animals/group. Tested compounds were administered orally once a day for 40 days. Glucose, triglycerides, and adiponectin results are day 40 values at end of study. [b] BW gain calculated from change in BW in each animal from day 0 to day 40. [c] Significantly different from time matched vehicle control, p < 0.05. [d] Significantly different from pioglitazone, p < 0.05.

dx.doi.org/10.1021/jm200409s |J. Med. Chem. 2011, 54, 4219–4233

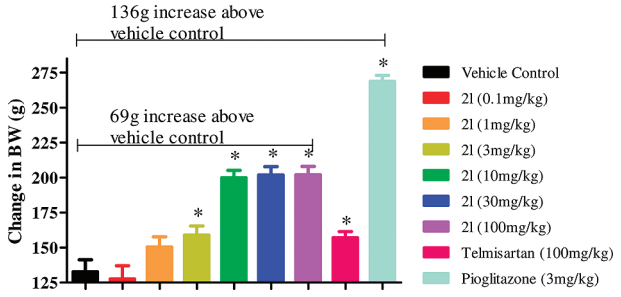

Figure 7. Effect of chronic (40 days) dosing of **2l** (0.1−100 mg/kg p.o.), telmisartan (100 mg/kg p.o.), and pioglitazone (3 mg/kg p.o.) on body weight gain in the 7 week old male ZDF rat. All data represented as mean ± SEM, n = 8 animals/group.

appeared to indicate a maximum effect on bodyweight despite improved efficacy on glucose and lipid end points. The weight gain due to drug, even at 100 mg/kg, was only 51% of that induced by pioglitazone (69 vs 136 g) reflecting the compound's partial agonist profile at the PPARγ receptor. The increase in adiponectin levels at doses of 10−100 mg/kg was equivalent to the effect of pioglitazone and, when viewed temporally, reflected a maintenance of baseline values rather than an acute increase. Therefore, as glycemic control decreased in vehicle control and low dose animals, adiponectin levels also declined whereas higher doses of **2l** and pioglitazone maintained both adiponectin levels and glycemic control. The relationship between adiponectin levels and glycemic control, either causal or association, was not investigated further in this model but did highlight the potential prognostic value of adiponectin as a biomarker for this mechanism of action.

A key question generated as a result of using two in vivo models was whether the projected PK/PD for the two biological activities overlapped, meaning that efficacy could be seen for both targets at similar plasma drug concentrations. In the SHR, the key steady-state plasma concentration required to lower BP was derived by comparing preclinical to clinical translation for telmisartan. The highest dose registered for telmisartan is 80 mg and was shown clinically to produce 90% of the maximal BP lowering observed in clinical trials. This provided a reference point that allowed translation of preclinical PK/PD and led us to model the preclinical EC_{90} for both telmisartan and **2l**. The steady-state free EC_{90} for **2l** in SHR was 7.2 nM. In the male ZDF rat, pioglitazone at 3 mg/kg was shown to produce a similar % maximal response in this preclinical model as the clinically used dose of 45 mg in human. Again, this dose and associated steady-state plasma concentration were used as the benchmark, and the steady-state free plasma concentration of **2l** that achieved similar efficacy was calculated to be 2.6 nM. On the basis of this modeling in two different disease models, plasma concentrations achieving significant efficacy were within 3-fold in the SHR and ZDF models for **2l** demonstrating the potential utility of this compound in treating multiple risk factors at a single dose level.

CONCLUSION

The current hypertension market is highly competitive and populated with many efficacious agents that have already or will soon lose market exclusivity. This makes the ability for an NCE to differentiate itself in such a market not just desirable but essential. The clustering of cardiovascular morbidities in what is often termed "metabolic syndrome" highlights the fact that hypertension rarely occurs in isolation and is often associated with other risk factors such as obesity, hypertriglyceridemia, and insulin resistance. The notion that a single molecule could start to address multiple risk factors provides a point of differentiation and potentially significant benefits to the "at risk" patient. Compound **2l** has demonstrated highly potent activity at two distinct molecular targets, a GPCR (AT1 receptor) and a nuclear hormone receptor (PPARγ). The combined beneficial effect of targeting these receptors has been demonstrated in two well-validated in vivo models of hypertension (SHR) and diabetes (ZDF). Compound **2l** demonstrated dual pharmacology with potent selective antagonism of the AT1 receptor that translated into highly effective BP lowering in the SHR. A single dose of 10 mg/kg produced BP lowering for a full 24 h equivalent to the most potent marketed ARB, telmisartan. It also displayed efficacy via partial agonism of the PPARγ receptor as demonstrated in cell based assays where E_{max} was only 20−30% of that seen with a reference TZD, darglitazone. This potent, partial activation translated into dose-dependent efficacy in the male ZDF rat with glycemic improvements equivalent to that of pioglitazone with a significantly reduced incidence of weight gain. A compound with a profile similar to **2l** should prove to be an attractive candidate for the treatment and prevention of type 2 diabetes and associated comorbidities such as hypertension and diabetic dyslipidemia.

EXPERIMENTAL SECTION

General. All chemicals, reagents, and solvents were purchased from commercial sources (e.g., Aldrich Chemical Co., Inc., Milwaukee, WI; Mallinckrodt Baker, Inc., Paris, KY, etc.) where available and used without further purification. All intermediates were characterized by proton nuclear magnetic spectroscopy (^{1}H NMR) and mass spectrometry (MS) using atmospheric pressure chemical ionization (APCI) or electron scatter (ES) ionization sources. All final compounds were determined to be consistent with the proposed structure by ^{1}H NMR and MS. All final compounds were purified by flash chromatography except where listed. HPLC conditions: method A: Symmetry C18, 4.6 × 150 mm; mobile phase: A: water + 0.1%TFA; B: CH_3CN + 0.1% TFA; flow rate: 1 mL/min; gradient: 90% A to 10% A in 15 min, hold for 5 min, go back to 90%A in 1 min and maintain at 90% A for 4 min; detection: DAD at 220 nm; injection volume: 10 uL; method A1: Phenomenex C18, 4.6 × 150 mm flow rate: 1 mL/min; gradient: 90% A to 10% A in 10 min; detection: DAD at 210 nm; injection volume: 10 uL. Chiral HPLC conditions (method B): chiralcel AS, 4.6 mm × 250 mm; mobile phase A: hexanes; B: isopropanol; isocratic 80:20; flow rate: 0.8 mL/min; injection volume: 10 μL; detection: DAD 214 nm. Purity of final compounds was determined by elemental analysis and HPLC. All final compounds were within theoretical limits for elemental analysis (CHN), unless noted.

*Synthesis of (S)-3-(5-(2-(1H-Tetrazol-5-yl)phenyl)-2,3-dihydro-1H-inden-1-yl)-5,7-dimethyl-2-propyl-3H-imidazo[4,5-b]pyridine (**2d**). Step 1. 2-Amino-4,6-dimethylnicotinamide (**4d**). General procedure **A**.* A solution of KOH (6.16 g, 110 mmol) in MeOH (100 mL) was treated sequentially with 2-amidino-acetamide hydrochloride (13.74 g, 99.88 mmol) and pentane-2,4-dione (10.29 mL, 99.88 mmol) and then stirred at room temperature for 24 h. Mixture diluted with water (50 mL) and cooled in ice bath to give white precipitate. Solid separated by filtration, washed with water, and dried in air overnight to give **4d** as a white solid (13.1 g, 79% yield): ^{1}H NMR (DMSO-d_6, 400 MHz) δ 7.58 (s, 1 H), 7.44 (s, 1 H), 6.24 (s, 1 H), 5.59 (s, 2 H), 2.14 (s, 3 H), 2.12 (s, 3 H); CIMS: 166.0 (APCI)+; 164.0 (APCI)-.

*Step 2. 5,7-Dimethyl-1H-imidazo[4,5-b]pyridin-2(3H)-one (**5d**). General procedure **B**.* A mixture of 2-amino-4,6-dimethylnicotinamide (**4d**) (9 g, 54.48 mmol) was added to solution of KOH (6.1 g, 56.106 mmol) in MeOH (150 mL). After cooling the mixture in an ice bath, $PhI(OAc)_2$ (17.55 g, 54.48 mmol) was added as a solid in small portions over 2 min. The mixture was stirred in an ice bath for 3 h, then warmed to room temperature and stirred overnight. The precipitate was collected by filtration, washed with ethyl ether, and air-dried to give **5d** as an off-white solid (8.39 g, 90% yield): ^{1}H NMR (DMSO-d_6, 400 MHz) δ 6.57 (s, 1 H), 2.26 (s, 3 H), 2.16 (s, 3 H); CIMS: 164.0 (APCI)+; 162.0 (APCI)-.

*Step 3. 5,7-Dimethyl-2-propyl-3H-imidazo[4,5-b]pyridine (**6d**). General procedure **C**.* 5,7-Dimethyl-1*H*-imidazo[4,5-*b*]pyridin-2(3*H*)-one (**5d**) (2.5 g, 15 mmol) was added to butyric anhydride (10 mL, 61.28 mmol) at room temperature under nitrogen. Butyric acid (5.6 mL, 61.28 mmol) was added followed by magnesium chloride (1.46 g, 15.32 mmol) as a solid. The mixture was then heated at 120 °C for 24 h. The reaction mixture was allowed to cool, and then MeOH (25 mL) was added. The mixture was heated at reflux for 4 h. Mixture allowed to cool, diluted with water (20 mL), and basified to approximately pH = 8. Mixture was partitioned between ethyl acetate (50 mL) and brine (50 mL). Phases separated. Aqueous phase was extracted with ethyl acetate (3 × 50 mL). The combined organic extracts were dried over magnesium sulfate and filtered and the solvent was removed. The residue was purified by MPLC on silica gel eluting with a gradient of ethyl acetate in hexanes (0% to 100%) to provide **6d** as an white solid (1.89 g, 65% yield): ^{1}H NMR (DMSO-d_6, 400 MHz) δ 12.40 (s, 1 H), 6.78 (s, 1 H), 2.71−2.68 (m, 2 H), 2.40 (s, 6 H), 1.71 (dt, J = 7.3 Hz, 2 H), 0.88 (t, J = 7.3 Hz, 3 H); CIMS: 190.0 (APCI)+; 188.1 (APCI)-. HPLC (method A): >99% purity; t_R = 7.404 min.

*Step 4. (R)-5-Bromo-2,3-dihydro-1H-inden-1-ol (**7**).* A solution of 5-bromo-1-indanone (15 g, 71.1 mmol) in anhydrous THF (120 mL) was stirred under nitrogen. A 1.0 M solution of (*S*)-methyl-CBS-oxazaborolidine in toluene (10.7 mL, 10.7 mmol) was added and the solution was warmed to 35 °C. A 2.0 M solution of borane-dimethylsulfide (46 mL, 92 mmol) was added dropwise over 90 min while maintaining the temperature at 35 °C for 1 h, then cooled to room temperature and stirred overnight. The mixture was cooled in ice bath, quenched with water (30 mL), and solvent removed. The mixture was extracted with ethyl acetate (3 × 150 mL). The combined organic extracts were washed with brine (100 mL), dried over magnesium sulfate, filtered, and concentrated. The residue was dissolved in chloroform (35 mL) at 50 °C. Hexanes (100 mL) were added slowly. Mixture was allowed to cool slowly to room temperature, and then further cooled in an ice bath. The white precipitate was separated by filtration, washed with hexanes, and dried to give **7** as white powder (8.95 g, 59%): ^{1}H NMR (DMSO-d_6, 400 MHz) δ 7.36 (s, 1 H), 7.30 (d, J = 8 Hz, 1 H), 7.20 (d, J = 8 Hz, 1 H), 4.93 (q, J = 6.3 Hz, 1 H), 2.88−2.82 (m, 1 H), 2.69−2.61 (m, 1 H), 2.30−2.22 (m, 1 H), 1.75−1.66 (m, 1 H). Chiral HPLC (method B): t_R (major enantiomer) = 6.583 min, t_R (minor enantiomer) = 5.672 min; >99% ee.

*Step 5. (R)-5-(2-(1-Trityl-1H-tetrazol-5-yl)phenyl)-2,3-dihydro-1H-inden-1-ol (**10**).* To a degassed solution of triphenylphosphine (0.12 g, 0.40 g, 0.44 mmol) in DME was added $Pd(OAc)_2$ (0.025 g, 0.11 mmol) and stirred for 10 min. To the reaction mixture was added boronic acid **9**[30] (0.50 g, 1.11 mmol), K_2CO_3 (0.38 g, 2.78 mmol), indanol **7** (0.24 g, 1.11 mmol), and water (0.05 mL, 2.78 mmol). The reaction mixture was heated at 110 °C overnight in a sealed tube. The solvent was removed under vacuum, and the residue was subjected to column chromatography (25% ethyl acetate in hexanes) to afford **10** (0.45 g, 89%): ^{1}H NMR (400 MHz, $CDCl_3$) δ 8.00 (d, J = 7.6 Hz, 1H), 7.59−6.90 (m, 22 H), 5.21−5.19 (m 1H), 2.85−2.79 (m, 1H), 2.62−2.55 (m, 1H), 2.44−2.38 (m, 1H), 1.90−1.80 (m, 1H).

*Step 6. (S)-5,7-Dimethyl-2-propyl-3-(5-(2-(1-trityl-1H-tetrazol-5-yl)-phenyl)-2,3-dihydro-1H-inden-1-yl)-3H-imidazo[4,5-b]pyridine (**11d**). General procedure **D**.* Indanol **10** (0.300 g, 0.576 mmol), imidazopyridine **6d** (0.22 g, 1.2 mmol), and triphenylphosphine (0.23 g, 0.86 mmol) were stirred in dry THF (20 mL) under a nitrogen atmosphere. Mixture cooled to 0 °C and a solution of DEAD (0.136 mL, 0.864 mmol) in THF (2 mL) was added dropwise. Mixture stirred overnight while allowing mixture to warm to RT. Mixture concentrated and purified by MPLC eluting with ethyl acetate in hexanes (0% to 20%) to afford as a colorless solid (0.208 g, 48% yield): CIMS: 692 (APCI)+; 448 (APCI)-. Product was taken to the next step without further characterization.

*Step 7. (S)-3-(5-(2-(1H-Tetrazol-5-yl)phenyl)-2,3-dihydro-1H-inden-1-yl)-5,7-dimethyl-2-propyl-3H-imidazo[4,5-b]pyridine (**2d**). General procedure **E**.* Trityl-protected tetrazol **11d** (0.205 g, 0.296 mmol) was dissolved in acetone (6 mL) and 3 M HCl (1 mL) was added. The mixture was stirred at room temperature for 3 h. Mixture was concentrated to give an aqueous residue that was cooled in an ice bath and basified with 2 N KOH to approximately pH 13. The resulting solid was separated by filtration and washed with water. The filtrate was extracted with diethyl ether (2 × 15 mL). The aqueous layer was cooled in an ice bath, and the pH adjusted to approximately pH 6.5 with 1.0 M HCl to give a cloudy solution. Mixture was extracted with chloroform (4 × 20 mL). The combined organic extracts were dried over magnesium sulfate, filtered, and the solvent evaporated. The resulting solid was dried under high vacuum to give **2d** as an off-white solid (25 mg, 19% yield): ^{1}H NMR (DMSO-d_6, 400 MHz) δ 7.66−7.60 (m, 2 H), 7.55−7.50 (m, 2 H), 7.11 (s, 1 H), 6.76 (d, J = 7.6 Hz, 1 H), 6.67 (d, J = 7.8 Hz, 1 H), 6.31 (bs, 1 H), 4.06−3.97 (m, 1 H), 3.23−3.18 (m, 1 H), 3.01−2.93 (m, 1 H), 2.64−2.63 (m, 3 H), 2.46 (s, 3 H), 2.43 (s, 3H), 1.87−1.66 (m, 3 H), 1.14 (m, 2 H), 0.84 (m, 3 H); CIMS: 450.2 (APCI)+; 448.1 (APCI)-; HPLC (method A): 98.57% purity; t_R = 10.62 min.

*Synthesis of (S)-3-(5-(2-(1H-Tetrazol-5-yl)phenyl)-2,3-dihydro-1H-inden-1-yl)-2-isopropyl-5,7-dimethyl-3H-imidazo[4,5-b]pyridine (**2f**). Step 1. 2-Isopropyl-5,7-dimethyl-3H-imidazo[4,5-b]pyridine (**6f**).* Prepared from **5d** (2.0 g, 12.3 mmol), isobutyric acid (4.54 mL, 49.03 mmol), and isobutyric anhydride (8.13 mL, 49.03 mmol) following General procedure **C**. **6f** was obtained as a pale yellow solid (0.92 g, 36% yield): ^{1}H NMR (DMSO-d_6, 400 MHz) δ 12.37 (s, 1 H), 6.78 (s, 1 H), 3.08−3.03 (m, 1 H), 2.44 (s, 3 H), 2.40 (s, 3 H); CIMS: 190.0 (APCI)+; 188.0 (APCI)-.

*Step 2. (S)-3-(5-Bromo-2,3-dihydro-1H-inden-1-yl)-2-isopropyl-5,7-dimethyl-3H-imidazo[4,5-b]pyridine (**8f**). General procedure **F**.* A mixture of indanol **7** (0.4 g, 1.88 mmol), imidazopyridine **6f** (0.53 g, 2.82 mmol), and triphenylphosphine (0.74 g, 2.82 mmol) in dry THF (20 mL) was stirred under nitrogen in an ice bath−brine in a Dewar flask (approximately −4 °C). A solution of DEAD (0.44 mL, 2.82 mmol) in THF (2 mL) was added slowly. The mixture was stirred in ice bath−brine for 5−6 h and then allowed to warm to room temperature and stirred overnight. Solvents were removed and the residue purified by MPLC on silica gel using a gradient of ethyl acetate in hexanes (0−14%). Pure fractions were combined and the solvent evaporated to give **8f** as a colorless foam (0.44 g, 61% yield): ^{1}H NMR (DMSO-d_6, 400 MHz) δ 7.52 (s, 1 H), 7.22 (d, J = 7.6 Hz, 1 H), 6.82 (s, 1 H), 6.68 (d, J = 8.1 Hz, 1 H), 6.24 (bs, 1 H), 3.23−3.20 (m, 2 H), 3.05−2.97 (m, 1 H), 2.44 (s, 3 H), 2.62−2.58 (m, 2 H), 2.44 (s, 3 H), 2.42 (s, 3 H), 1.28 (d, J = 6.6 Hz, 3 H), 1.12 (m, 3 H); CIMS: 385.9 (APCI)+; 383.9 (APCI)-; HPLC (method A): 98.2% purity; t_R = 12.2 min.

*Step 3. (S)-2-Isopropyl-5,7-dimethyl-3-(5-(2-(1-trityl-1H-tetrazol-5-yl)phenyl)-2,3-dihydro-1H-inden-1-yl)-3H-imidazo[4,5-b]pyridine (**11f**). General procedure **G**.* Palladium(II) acetate (25.4 mg, 0.113 mmol) was added to a degassed solution of triphenylphosphine (118 mg, 0.452 mmol) in dry DME (10 mL). The mixture was stirred at room temperature for 20 min. Boronic acid **9** (0.63 g, 1.5 mmol), a solution of bromide **8f** (0.43 g, 1.13 mmol) in dry DME (5 mL), K_2CO_3 (0.39 g, 2.82 mmol), and water (0.051 mL) were added. The mixture was degassed for an additional 30 min, and then heated at 80 °C overnight. Mixture was allowed to cool, diluted with ethyl acetate, and silica gel was

added. Solvents were removed and the residue was purified by MPLC on silica gel using a gradient of ethyl acetate in hexanes (0−20%). Pure fractions were combined and evaporated to give **11f** as an off-white foam (0.65 g., 81% yield): CIMS: 692.3 (APCI)+; 448.2 (APCI)-; HPLC (method A): 97% purity; t_R = 16.31 min; product was taken to the next step without further characterization.

*Step 4. (S)-3-(5-(2-(1H-Tetrazol-5-yl)phenyl)-2,3-dihydro-1H-inden-1-yl)-2-isopropyl-5,7-dimethyl-3H-imidazo[4,5-b]pyridine (**2f**).* Prepared from trityl-protected tetrazole **11f** (0.64 g, 0.93 mmol) following general procedure **E** to provide **11f** as a white solid (0.35 g, 86% yield): ^{1}H NMR (DMSO-d_6, 400 MHz) δ 7.64−7.57 (m, 2 H), 7.52−7.48 (m, 2 H), 7.12 (s, 1 H), 6.83 (s, 1 H), 6.71 (d, J = 7.8 Hz, 1 H), 6.63 (d, J = 7.8 Hz, 1 H), 6.35 (bs, 1 H), 3.26−3.10 (m, 1 H), 3.00−2.92 (m, 1 H), 2.64−2.58 (m, 1 H), 2.44 (s, 3 H), 2.42 (s, 3 H), 2.35 (bs, 2 H), 1.26 (bs, 3 H), 1.04 (m, 3 H); CIMS: 448.2 (APCI)-; HPLC (method A): >99% purity; t_R = 10.59 min; Anal. Calcd for $C_{27}H_{27}N_7 \cdot 1.0\ H_2O$: C, 69.36; H, 6.25; N, 20.97. Found: C, 69.71; H, 5.89; N, 20.57.

*Synthesis of (S)-3-(5-(2-(1H-Tetrazol-5-yl)phenyl)-2,3-dihydro-1H-inden-1-yl)-2-cyclopropyl-5,7-dimethyl-3H-imidazo[4,5-b]pyridine (**2g**). Step 1. (S)-2-Cyclopropyl-5,7-dimethyl-3-(5-(2-(1-trityl-1H-tetrazol-5-yl)phenyl)-2,3-dihydro-1H-inden-1-yl)-3H-imidazo[4,5-b]pyridine (**11g**).* Prepared from imidazopyridine **6g**[45] (0.108 g, 0.576 mmol) following general procedure **D** to provide **11g** as a white solid (76 mg, 35%): CIMS: 690.1 (APCI)+; 446.1 (APCI)-. Product was taken to the next step without further characterization.

*Step 2. (S)-3-(5-(2-(1H-Tetrazol-5-yl)phenyl)-2,3-dihydro-1H-inden-1-yl)-2-cyclopropyl-5,7-dimethyl-3H-imidazo[4,5-b]pyridine (**2g**).* Prepared from trityl-protected tetrazole **11g** (72 mg, 0.104 mmol) following General procedure **E** to provide **2g** as a white solid (35 mg, 83% yield): ^{1}H NMR (DMSO-d_6, 400 MHz) δ 7.65−7.59 (m, 2 H), 7.53−7.50 (m, 2 H), 7.11 (s, 1 H), 6.84 (s, 1 H), 6.74 (s, 2 H), 6.49 (t, J = 8.4 Hz, 1 H), 3.16−3.14 (m, 1 H), 3.02−2.94 (m, 1 H), 2.71−2.61 (m, 2 H), 2.53−2.48 (m, 1 H), 2.44 (s, 3 H), 2.38 (s, 3 H), 0.94−0.90 (m, 3 H), 0.89−0.74 (m, 1 H); CIMS: 448.0 (APCI)+, 446.1 (APCI)-; HPLC (method A): 99.39% purity; t_R = 10.51 min.

*Synthesis of (S)-3-(5-(2-(1H-Tetrazol-5-yl)phenyl)-2,3-dihydro-1H-inden-1-yl)-2-ethyl-5,6,7-trimethyl-3H-imidazo[4,5-b]pyridine (**2h**). Step 1. 2-Amino-4,5,6-trimethylnicotinamide (**4h**).* Prepared from 2-amidinoacetamide hydrochloride (12.05 g, 87.61 mmol) and 3-methylpentane-2,4-dione (10 g, 87.61 mmol) following general procedure **A**. Nicotinamide **4h** was obtained as an off-white solid (7.48 g, 77% yield): ^{1}H NMR (DMSO-d_6, 400 MHz) δ 7.60 (s, 1 H), 7.42 (s, 1 H), 5.20 (s, 2 H), 2.19 (s, 3 H), 2.06 (s, 3 H), 1.95 (s, 3 H); CIMS: 180.0 (APCI)+; 178.0 (APCI)-.

*Step 2. 5,6,7-Trimethyl-1H-imidazo[4,5-b]pyridin-2(3H)-one (**5h**).* Prepared from nicotinamide **4h** (7.48 g, 41.7 mmol) following general procedure **B**. **5h** was obtained as an greyish solid (3.16 g, 43% yield): ^{1}H NMR (DMSO-d_6, 400 MHz) δ 10.83 (bs, 1 H), 10.60 (bs, 1 H), 2.28 (s, 3 H), 2.14 (s, 3 H), 2.04 (s, 3 H); CIMS: 178.0 (APCI)+; 176.0 (APCI)-.

*Step 3. 2-Ethyl-5,6,7-trimethyl-3H-imidazo[4,5-b]pyridine (**6h**).* Prepared from **5h** (1.65 g, 9.3 mmol), propionic acid (2.8 mL, 37.2 mmol), and propionic anhydride (4.80 mL, 37.2 mmol) following general procedure **C**. **6h** was obtained as an off-white solid (1.24 g, 70% yield): ^{1}H NMR (DMSO-d_6, 400 MHz) δ 12.23 (s, 1 H), 2.72 (q, J = 7.6 Hz, 2 H), 2.44 (s, 3 H), 2.40 (s, 3 H), 2.15 (s, 3 H), 1.23 (t, J = 7.6 Hz, 3 H); CIMS: 190.0 (APCI)+; 188.0 (APCI)-.

*Step 4. (S)-3-(5-Bromo-2,3-dihydro-1H-inden-1-yl)-2-ethyl-5,6,7-trimethyl-3H-imidazo[4,5-b]pyridine (**8h**).* Prepared from imidazopyridine **6h** (0.53 g, 2.82 mmol) following general procedure **F** to give **8h** (0.42 g, 58% yield): ^{1}H NMR (DMSO-d_6, 400 MHz) δ 7.51 (s, 1 H), 7.22 (d, J = 8 Hz, 1 H), 6.69 (d, J = 8.5 Hz, 1 H), 6.17 (bs, 1 H), 3.04−2.96 (m, 1 H), 2.73 (bs, 1 H), 2.63−2.55 (m, 3 H), 2.44 (s, 3 H), 2.32 (s, 3 H), 2.13 (s, 3 H), 1.20 (t, J = 7.6 Hz, 3 H); CIMS: 386.1 (APCI)+; 384 (APCI)-; HPLC (method A): 97.95% purity; t_R = 12.338 min.

*Step 5. (S)-2-Ethyl-5,6,7-trimethyl-3-(5-(2-(1-trityl-1H-tetrazol-5-yl)-phenyl)-2,3-dihydro-1H-inden-1-yl)-3H-imidazo[4,5-b]pyridine (**11h**).* Prepared from bromide **8h** (0.42 g, 1.09 mmol) following general procedure **G**. **11h** was obtained as a foam (0.67 g., 85% yield): CIMS: 692.4 (APCI)+; 448.2 (APCI)-. Product was taken to the next step without further characterization.

*Step 6. (S)-3-(5-(2-(1H-Tetrazol-5-yl)phenyl)-2,3-dihydro-1H-inden-1-yl)-2-ethyl-5,6,7-trimethyl-3H-imidazo[4,5-b]pyridine (**2h**).* Prepared from trityl-protected tetrazole **11h** (0.67 g, 0.973 mmol) following general procedure **E**. Tetrazole **2h** was obtained as a white solid (0.325 g, 77% yield): ^{1}H NMR (DMSO-d_6, 400 MHz) δ 7.63−7.59 (m, 2 H), 7.57−7.48 (m, 2 H), 7.08 (s, 1 H), 6.72 (d, J = 7.8 Hz, 1 H), 6.64 (d, J = 8 Hz, 1 H), 6.26 (bs, 1 H), 2.98−2.90 (m, 1 H), 2.64−2.57 (m, 2 H), 2.44 (s, 3 H), 2.36 (s, 3 H), 2.15 (s, 3 H), 1.17 (t, J = 7.3 Hz, 3 H); CIMS: 450.2 (APCI)+; 448.1 (APCI)-; HPLC (method A): >98% purity; t_R = 10.73 min. Anal. Calcd for $C_{27}H_{27}N_7 \cdot 0.15$ EtOAc: C, 71.63; H, 6.14; N, 21.19. Found: C, 71.26; H, 6.05; N, 21.01.

*Synthesis of (S)-3-(5-(2-(1H-Tetrazol-5-yl)phenyl)-2,3-dihydro-1H-inden-1-yl)-2,6-diethyl-5,7-dimethyl-3H-imidazo[4,5-b]pyridine (**2i**). Step 1. 2-Amino-5-ethyl-4,6-dimethylnicotinamide (**4i**).* Prepared from 2-amidino-acetamide hydrochloride (3.22 g, 23.41 mmol) and 3-ethylpentane-2,4-dione (3 g, 23.41 mmol) following general procedure **A**. Nicotinamide **4i** was obtained as an off-white solid (1.39 g, 31% yield): ^{1}H NMR (DMSO-d_6, 400 MHz) δ 7.62 (s, 1 H), 7.42 (s, 1 H), 5.20 (s, 2 H), 2.42 (q, J = 7.4 Hz, 2 H), 2.21 (s, 3 H), 2.10 (s, 3 H), 0.96 (t, J = 7.4 Hz, 3 H); CIMS: 194.0 (APCI)+; 192.0 (APCI)-.

*Step 2. 6-Ethyl-5,7-dimethyl-1H-imidazo[4,5-b]pyridin-2(3H)-one (**5i**).* Prepared from nicotinamide **4i** (1.2 g, 6.2 mmol) following general procedure **B**. **5i** was obtained as a solid (1.11 g, 94% yield): ^{1}H NMR (DMSO-d_6, 400 MHz) δ 2.51 (q, J = 7.6 Hz, 2 H), 2.31 (s, 3 H), 2.17 (s, 3 H), 0.98 (q, J = 7.6 Hz, 3 H); CIMS: 192.0 (APCI)+; 190.0 (APCI)-.

*Step 3. 2,6-Diethyl-5,7-dimethyl-3H-imidazo[4,5-b]pyridine (**6i**).* Prepared from **5i** (0.6 g, 3.138 mmol), propionic acid (0.94 mL, 12.55 mmol), and propionic anhydride (1.62 mL, 12.55 mmol) following general procedure **C**. **6i** was obtained as an off-white solid (0.335 g, 52% yield): ^{1}H NMR (DMSO-d_6, 400 MHz) δ 12.24 (s, 1 H), 2.72 (q, J = 7.6 Hz, 2 H), 2.62 (q, J = 7.6 Hz, 2 H), 2.44 (s, 6 H), 1.23 (t, J = 7.6 Hz, 3 H), 1.02 (t, J = 7.6 Hz, 3 H); CIMS: 204.0 (APCI)+; 202.1 (APCI)-.

*Step 4. (S)-3-(5-Bromo-2,3-dihydro-1H-inden-1-yl)-2,6-diethyl-5,7-dimethyl-3H-imidazo[4,5-b]pyridine (**8i**).* Prepared from imidazopyridine **6i** (0.335 g, 1.648 mmol) following general procedure **F** to give **8i** as a yellow oil (0.36 g, 54% yield): ^{1}H NMR (DMSO-d_6, 400 MHz) δ 7.52 (s, 1 H), 7.22 (d, J = 8 Hz, 1 H), 6.72 (d, J = 8 Hz, 1 H), 6.18 (bs, 1 H), 3.11−2.96 (m, 1 H), 2.74−2.70 (m, 1 H), 2.62−2.58 (m, 2 H), 2.44 (s, 3 H), 1.20 (t, J = 7.3 Hz, 3 H), 1.01 (t, J = 7.6 Hz, 3 H); CIMS: 398.1 (APCI)+.

*Step 5. (S)-2,6-Diethyl-5,7-dimethyl-3-(5-(2-(1-trityl-1H-tetrazol-5-yl)phenyl)-2,3-dihydro-1H-inden-1-yl)-3H-imidazo[4,5-b]pyridine (**11i**).* Prepared from bromide **8i** (0.36 g, 0.898 mmol) following general procedure **G**. **11i** was obtained as a white foam (0.389 g, 61% yield): CIMS: 706.3 (APCI)+; 462.1 (APCI)-. Product was taken to the next step without further characterization.

*Step 6. (S)-3-(5-(2-(1H-Tetrazol-5-yl)phenyl)-2,3-dihydro-1H-inden-1-yl)-2,6-diethyl-5,7-dimethyl-3H-imidazo[4,5-b]pyridine (**2i**).* Prepared from trityl-protected tetrazole **11i** (0.389 g, 0.551 mmol) following general procedure **E**. Tetrazole **2i** was obtained as a white foam (61 mg, 24% yield): ^{1}H NMR (DMSO-d_6, 400 MHz) δ 7.63−7.58 (m, 2 H), 7.52−7.48 (m, 2 H), 7.08 (s, 1 H), 6.73 (d, J = 7.8 Hz, 1 H), 6.67 (d, J = 8 Hz, 1 H), 6.26 (bs, 1 H), 2.98−2.90 (m, 1 H), 2.63 (q, J = 7.3 Hz, 4 H), 2.44 (s, 3 H), 1.17 (t, J = 7.3 Hz, 3 H), 1.02 (t, J = 7.3 Hz, 3 H); CIMS: 450.2 (APCI)+; 448.1 (APCI)-; HPLC (method A): 92.79% purity; t_R = 11.232 min.

*Synthesis of (S)-3-(5-(2-(1H-Tetrazol-5-yl)phenyl)-2,3-dihydro-1H-inden-1-yl)-2,5-diethyl-7-methyl-3H-imidazo[4,5-b]pyridine (**2j**). Step 1.*

*2-Amino-6-ethyl-4-methylnicotinamide (**4j**).* Prepared from 2-amidinoacetamide hydrochloride (12.05 g, 87.61 mmol) and hexane-2,4-dione (10 g, 87.61 mmol) following general procedure **A**. Nicotinamide **4j** was obtained as an off-white solid (12.98 g, 83% yield): ^{1}H NMR (DMSO-d_6, 400 MHz, major isomer) δ 7.59 (s, 1 H), 7.44 (s, 1 H), 6.25 (s, 1 H), 5.57 (s, 2 H), 2.44 (q, J = 7.6 Hz, 2 H), 2.13 (s, 3 H), 1.08 (d, J = 7.6 Hz, 3 H); MS: 180.0 (APCI)+; 178.0 (APCI)-.

*Step 2. 5-Ethyl-7-methyl-1H-imidazo[4,5-b]pyridin-2-(3H)-one (**5j**).* Prepared from nicotinamide **4j** (7.85 g, 43.8 mmol) following general procedure **B**. **5j** was obtained as an off-white solid (6.74 g, 87% yield): ^{1}H NMR (DMSO-d_6, 400 MHz) δ 10.90 (bs, 2 H), 6.58 (s, 1 H), 2.54 (q, J = 7.6 Hz, 2 H), 2.17 (s, 3 H), 1.12 (t, J = 7.6 Hz, 3 H); CIMS: 178.0 (APCI)+; 176.0 (APCI)-.

*Step 3. 2,5-Diethyl-7-methyl-3H-imidazo[4,5-b]pyridine (**6j**).* Prepared from **5j** (2.0 g, 11.3 mmol), propionic acid (3.37 mL, 45.15 mmol), and propionic anhydride (5.82 mL, 45.15 mmol) following general procedure **C**. **6j** was obtained as a yellow solid (1.40 g, 65% yield): ^{1}H NMR (DMSO-d_6, 400 MHz) δ 12.41 (s, 1 H), 6.79 (s, 1 H), 2.74 (q, J = 7.6 Hz, 2 H), 2.68 (q, J = 7.6 Hz, 2 H), 2.41 (s, 3 H), 1.25 (t, J = 7.6 Hz, 3 H), 1.18 (t, J = 7.6 Hz, 7 H); CIMS: 190.0 (APCI)+; 188.0 (APCI)-.

*Step 4. (S)-2-Ethyl-5,7-dimethyl-3-(5-(2-(1-trityl-1H-tetrazol-5-yl)-phenyl)-2,3-dihydro-1H-inden-1-yl)-3H-imidazo[4,5-b]pyridine (**11j**).* Prepared from imidazopyridine **6j** (0.172 g, 0.910 mmol) following general procedure **D** to provide **11j** as colorless solid (0.107 g, 31% yield): CIMS: 629.1 (APCI)+; 448.1 (APCI)-. Product was taken to the next step without further characterization.

*Step 5. (S)-3-(5-(2-(1H-Tetrazol-5-yl)phenyl)-2,3-dihydro-1H-inden-1-yl)-2,5-diethyl-7-methyl-3H-imidazo[4,5-b]pyridine (**2j**).* Prepared from trityl-protected tetrazole **11j** (0.103 g, 0.149 mmol) following general procedure **E**. Tetrazole **2j** was obtained as a white solid (44 mg, 73% yield): ^{1}H NMR (DMSO-d_6, 400 MHz) δ 7.64−7.57 (m, 2 H), 7.53−7.46 (m, 2 H), 7.00 (s, 1 H), 6.82 (s, 1 H), 6.72 (d, J = 9.0 Hz, 1 H), 6.67 (d, J = 7.8 Hz, 1 H), 6.28 (bs, 1 H), 2.99−2.91 (m, 1 H), 2.77−2.48 (m, 4 H), 2.43 (s, 3 H), 1.19 (t, J = 7.3 Hz, 3 H), 1.07 (t, J = 7.3 Hz, 3 H); CIMS: (APCI)+; (APCI)-. HPLC (method A): 95.42% purity; t_R = 10.979 min. Anal. Calcd for $C_{27}H_{27}N_7$·0.31 EtOAc: C, 71.13; H, 6.23; N, 20.56. Found: C, 70.83; H, 6.24; N, 20.18.

*Synthesis of (S)-3-(5-(2-(1H-Tetrazol-5-yl)phenyl)-2,3-dihydro-1H-inden-1-yl)-5-ethyl-2-isopropyl-7-methyl-3H-imidazo[4,5-b]pyridine (**2k**). Step 1. 5-Ethyl-2-isopropyl-7-methyl-3H-imidazo[4,5-b]pyridine (**6k**).* Prepared from **5j** (2.0 g, 11.3 mmol), isobutyric acid (4.19 mL, 45.15 mmol), and isobutyric anhydride (7.48 mL, 45.15 mmol) following general procedure **C**. **6k** was obtained as a yellow solid (1.85 g, 81% yield): ^{1}H NMR (DMSO-d_6, 400 MHz) δ 12.41 (s, 1 H), 6.80 (s, 1 H), 3.10−3.01 (m, 1 H), 2.68 (q, J = 7.6 Hz, 2 H), 2.44 (s, 3 H), 1.27 (d, J = 6.8 Hz, 6 H), 1.18 (t, J = 7.6 Hz, 3 H); CIMS: 204.0 (APCI)+; 202.1 (APCI)-.

*Step 2. (S)-3-(5-Bromo-2,3-dihydro-1H-inden-1-yl)-5-ethyl-2-isopropyl-7-methyl-3H-imidazo[4,5-b]pyridine (**8k**).* Prepared from imidazopyridine **6k** (0.57 g, 2.82 mmol) following general procedure **F** to give **8k** (0.37 g, 50% yield): ^{1}H NMR (DMSO-d_6, 400 MHz) δ 7.51 (s, 1 H), 7.20 (d, J = 7.3 Hz, 1 H), 6.80 (s, 1 H), 6.68 (d, J = 8.0 Hz, 1 H), 6.21 (bs, 1 H), 3.07−2.97 (m, 1 H), 2.67−2.47 (m, 5 H), 2.44 (s, 3 H), 1.31 (d, J = 6.6 Hz, 3 H), 1.17 (s, 3 H), 1.00 (s, 3 H); CIMS: 400.0 (APCI)+; 398.1 (APCI)-; HPLC (method A): >99% purity; t_R = 13.038 min.

*Step 3. (S)-5-Ethyl-2-isopropyl-7-methyl-3-(5-(2-(1-trityl-1H-tetrazol-5-yl)phenyl)-2,3-dihydro-1H-inden-1-yl)-3H-imidazo[4,5-b]pyridine (**11k**).* Prepared from bromide **8k** (0.38 g, 0.944 mmol) following general procedure **G**. **11k** was obtained as a pale yellow oil (0.548 g., 81% yield): CIMS: 706.4 (APCI)+; 462.3 (APCI)-. Product was taken to the next step without further characterization.

*Step 4. (S)-3-(5-(2-(1H-Tetrazol-5-yl)phenyl)-2,3-dihydro-1H-inden-1-yl)-5-ethyl-2-isopropyl-7-methyl-3H-imidazo[4,5-b]pyridine (**2k**).* Prepared from trityl-protected tetrazole **11k** (0.548 g, 0.776 mmol) following general procedure **E**. Tetrazole **2k** was obtained as an off-white solid (0.21 g, 60% yield): ^{1}H NMR (DMSO-d_6, 400 MHz) δ 7.63−7.57 (m, 2 H), 7.52−7.44 (m, 2 H), 7.10 (s, 1 H), 6.81 (s, 1 H), 6.71 (d, J = 7.8 Hz, 1 H), 6.64 (d, J = 7.8 Hz, 1 H), 6.29 (bs, 1 H), 3.00−2.92 (m, 1 H), 2.61−2.45 (m, 3 H), 2.44 (s, 3 H), 1.29 (d, J = 6.3 Hz, 3 H), 1.22−0.95 (m, 6 H); CIMS: 464.3 (APCI)+; 462.2 (APCI)-; HPLC (method A): >99% purity; t_R = 11.26 min. Anal. Calcd for $C_{29}H_{29}N_7$·0.14 EtOAc: C, 72.06; H, 6.38; N, 20.60. Found: C, 72.35; H, 6.47; N, 20.23.

*Synthesis of (S)-3-(5-(2-(1H-Tetrazol-5-yl)phenyl)-2,3-dihydro-1H-inden-1-yl)-2-ethyl-5-isobutyl-7-methyl-3H-imidazo[4,5-b]pyridine (**2l**). Step 1. 2-Amino-6-isobutyl-4-methyl-nicotinamide (**4l**).* Prepared from 6-methylheptane-2,4-dione (5 g, 35.2 mmol) following general procedure **A**. These conditions provided an approximately 86:14 mixture of 2-amino-6-isobutyl-4-methyl-nicotinamide (major isomer) and 2-amino-4-isobutyl-6-methyl-nicotinamide (minor isomer) as determined by ^{1}H NMR that was not separated. Mixture was obtained as an off-white solid (3.83 g, 53% yield): ^{1}H NMR (DMSO-d_6, 400 MHz, major isomer) δ 7.60 (s, 1 H), 7.44 (s, 1 H), 6.21 (s, 1 H), 5.57 (s, 2 H), 2.25 (d, J = 7.2 Hz, 2 H), 2.13 (s, 3 H), 1.96−1.89 (m, 1 H), 0.81 (d, J = 6.6 Hz, 6 H); CIMS: 208.0 (APCI)+; 206.1 (APCI)-.

*Step 2. 5-Isobutyl-7-methyl-1,3-dihydro-imidazo[4,5-b]pyridin-2-one (**5l**).* Prepared from the mixture of 2-amino-6-isobutyl-4-methyl-nicotinamide (**4l**) and 2-amino-4-isobutyl-6-methyl-nicotinamide (3.8 g, 18.3 mmol) following general procedure **B**. These conditions provided an approximately 86:14 mixture of 5-isobutyl-7-methyl-1,3-dihydro-imidazo[4,5-*b*]pyridin-2-one (**5l**, major isomer) and 7-isobutyl-5-methyl-1,3-dihydro-imidazo[4,5-*b*]pyridin-2-one (minor isomer) that was not separated. Mixture was obtained as an off-white solid (2.62 g, 70% yield): ^{1}H NMR (DMSO-d_6, 400 MHz, major isomer) δ 10.98 (s, 1 H), 10.71 (s, 1 H), 6.54 (s, 1 H), 2.38 (d, J = 7.3 Hz, 2 H), 2.17 (s, 3 H), 1.95−1.88 (m, 1 H), 0.79 (d, J = 6.8 Hz, 6 H); CIMS: 206.0 (APCI)+; 204.0 (APCI)-.

*Step 3. 2-Ethyl-5-isobutyl-7-methyl-3H-imidazo[4,5-b]pyridine (**6l**).* Prepared from the approximately the mixture of 5-isobutyl-7-methyl-1,3-dihydro-imidazo[4,5-*b*]pyridin-2-one (**5l**) and 7-isobutyl-5-methyl-1,3-dihydro-imidazo[4,5-*b*]pyridin-2-one (1.0 g, 4.87 mmol), propionic acid (1.45 mL, 19.5 mmol), and propionic anhydride (2.51 mL, 19.5 mmol) following general procedure **C**. These conditions provided an approximately 86:14 mixture of 2-ethyl-5-isobutyl-7-methyl-3*H*-imidazo[4,5-*b*]pyridine (**6l**, major product) and 2-ethyl-7-isobutyl-5-methyl-3*H*-imidazo[4,5-*b*]pyridine as an off-white solid (0.93 g, 88% yield): ^{1}H NMR (DMSO-d_6, 400 MHz, major isomer) δ 12.41 (s, 1 H), 6.75 (s, 1 H), 2.80−2.71 (m, 2 H), 2.52 (d, J = 7.2 Hz, 2 H), 2.41 (s, 3 H), 2.03−1.96 (m, 1 H), 1.24 (t, J = 7.6 Hz, 3 H), 0.82 (d, J = 6.6 Hz, 6 H); CIMS: 218.0 (APCI)+; 216.1 (APCI)-. HPLC (method A) showed two compounds: (major component): 86% area; t_R = 9.095 min; (minor component): 14% area; t_R = 8.735 min.

*Step 4. (S)-3-(5-Bromo-2,3-dihydro-1H-inden-1-yl)-2-ethyl-5-isobutyl-7-methyl-3H-imidazo[4,5-b]pyridine (**8l**).* Prepared from the mixture of imidazopyridine **6l** and corresponding regioisomer (0.61 g, 2.82 mmol) following general procedure **F** to give **8l** (0.4 g, 52% yield): ^{1}H NMR (DMSO-d_6, 400 MHz) δ 7.49 (s, 1 H), 7.18 (d, J = 8.05 Hz, 1 H), 6.74 (s, 1 H), 6.70 (d, J = 8.05 Hz, 1 H), 6.15 (bs, 1 H), 3.04−2.96 (m, 1 H), 2.83−2.48 (m, 5 H), 2.44 (s, 3 H), 1.83−1.76 (m, 1 H), 1.25 (t, J = 7.6 Hz, 3 H), 0.67 (dd, J = 15.4, 6.6 Hz, 6 H); CIMS: 412.0 (APCI)+; 412.0 (APCI)-; HPLC (method A): 93.89% purity; t_R = 13.925 min.

*Step 5. (S)-2-Ethyl-5-isobutyl-7-methyl-3-(5-(2-(1-trityl-1H-tetrazol-5-yl)phenyl)-2,3-dihydro-1H-inden-1-yl)-3H-imidazo[4,5-b]pyridine (**11l**).* Prepared from bromide **8l** (0.39 g, 0.948 mmol) following general procedure **G**. **11l** was obtained as a pale yellow oil (0.56 g., 72% yield): CIMS: 720.4 (APCI)+; 476.2 (APCI)-. Product was taken to the next step without further characterization.

Step 6. (S)-3-(5-(2-(1H-Tetrazol-5-yl)phenyl)-2,3-dihydro-1H-inden-1-yl)-2-ethyl-5-isobutyl-7-methyl-3H-imidazo[4,5-b]pyridine

(2l). Prepared from trityl-protected tetrazole **11l** (0.55 g, 0.764 mmol) following general procedure **E**. Tetrazole **2l** was obtained as an off-white solid (0.24 g, 75% yield): ^{1}H NMR (DMSO-d_6, 400 MHz) δ 7.64−7.57 (m, 2 H), 7.52−7.43 (m, 2 H), 7.07 (s, 1 H), 6.76 (s, 1 H), 6.71 (d, J = 8.05 Hz, 1 H), 6.65 (d, J = 7.8 Hz, 1 H), 6.24 (bs, 1 H), 2.98−2.90 (m, 1 H), 2.75 (m, 1 H), 2.66−2.58 (m, 2 H), 2.41 (s, 3 H), 1.86−1.83 (m, 1 H), 1.21 (t, J = 7.3 Hz, 3 H), 0.71 (t, J = 6.8 Hz, 6 H); CIMS: 478.2 (APCI)+; 476.3 (APCI)-; HPLC (method A): >99% purity; t_R = 12.04 min. Chiral HPLC (SFC conditions): chiralpak AD-H, 4.6 mm × 250 mm; mobile phase: 80/20 CO_2/MeOH; gradient: isocratic; flow rate: 2.5 mL/min; injection volume: 10 μL; detection: UV at 210 nm; t_R (major enantiomer) = 4.97 min, t_R (minor enantiomer) = 3.89 min; 96.5%ee. Anal. Calcd for $C_{29}H_{31}N_7 \cdot 0.48\ H_2O$: C, 71.63; H, 6.62; N, 20.16. Found: C, 71.58; H, 6.43; N, 19.77.

*Synthesis of (S)-3-(5-(2-(1H-Tetrazol-5-yl)phenyl)-2,3-dihydro-1H-inden-1-yl)-5-isobutyl-2-isopropyl-7-methyl-3H-imidazo[4,5-b]pyridine (**2m**). Step 1. 5-Isobutyl-2-isopropyl-7-methyl-3H-imidazo[4,5-b]pyridine (**6m**).* Prepared from the mixture of 5-isobutyl-7-methyl-1,3-dihydro-imidazo[4,5-*b*]pyridin-2-one (**5l**) and 7-isobutyl-5-methyl-1,3-dihydro-imidazo[4,5-*b*]pyridin-2-one (1.0 g, 4.87 mmol), isobutyric acid (1.81 mL, 19.49 mmol), and isobutyric anhydride (3.23 mL, 19.49 mmol) following general procedure **C**. These conditions provided **6m** as an off-white foam (0.68 g, 56% yield): ^{1}H NMR (DMSO-d_6, 400 MHz, major isomer) δ 6.75 (s, 1 H), 3.10−3.01 (m, 1 H), 2.52 (d, J = 7.2 Hz, 2 H), 2.44 (s, 3 H), 2.04−1.97 (m, 1H), 1.27 (d, J = 7 Hz, 6 H), 0.82 (d, J = 6.6 Hz, 6 H); CIMS: 232.1 (APCI)+; 230.1 (APCI)-.

*Step 2. (S)-3-(5-Bromo-2,3-dihydro-1H-inden-1-yl)-5-isobutyl-2-isopropyl-7-methyl-3H-imidazo[4,5-b]pyridine (**8m**).* Prepared from imidazopyridine **6m** (0.42 g, 1.80 mmol) following general procedure **F** to afford **8m** as a white solid (0.24 g, 41% yield): ^{1}H NMR (DMSO-d_6, 400 MHz) δ 7.49 (s, 1 H), 7.17 (d, J = 7.6 Hz, 1 H), 6.73 (s, 3 H), 6.65 (d, J = 8 Hz, 1 H), 6.18 (bs, 1 H), 3.06−2.96 (m, 1 H), 2.66−2.40 (m, 6 H), 2.41 (s, 3 H), 1.76 (m, 1 H), 1.34−1.21 (m, 6 H), 0.67−0.61 (m, 6 H); CIMS: 428.1 (APCI)+; 426.1 (APCI)-; HPLC (method A): >99% purity; t_R = 14.27 min.

*Step 3. (S)-5-Isobutyl-2-isopropyl-7-methyl-3-(5-(2-(1-trityl-1H-tetrazol-5-yl)phenyl)-2,3-dihydro-1H-inden-1-yl)-3H-imidazo[4,5-b]pyridine (**11m**).* Prepared from bromide **8m** (0.24 g, 0.56 mmol) following general procedure **G**. **11m** was obtained as a colorless solid (0.35 g., 85% yield): CIMS: 734.2 (APCI)+; 492.0 (APCI)-. Product was taken to the next step without further characterization.

*Step 4. (S)-3-(5-(2-(1H-Tetrazol-5-yl)phenyl)-2,3-dihydro-1H-inden-1-yl)-5-isobutyl-2-isopropyl-7-methyl-3H-imidazo[4,5-b]pyridine (**2m**).* Prepared from trityl-protected tetrazole **11m** (0.35 g, 0.48 mmol) following general procedure **E**. Tetrazole **2m** was obtained as a white solid (0.19 g, 79% yield): ^{1}H NMR (DMSO-d_6, 400 MHz) δ 7.63−7.56 (m, 2 H), 7.51−7.47 (m, 1 H), 7.42 (d, J = 7.6 Hz, 1 H), 7.09 (s, 1 H), 6.74 (s, 1 H), 6.69 (d, J = 7.8 Hz, 1 H), 6.61 (d, J = 7.8 Hz, 1 H), 6.26 (bs, 1 H), 2.99−2.91 (m, 1 H), 2.61 (m, 1 H), 2.41 (s, 3 H), 1.80 (m, 1 H), 1.31−1.10 (m, 6 H), 0.69 (m, 6 H); CIMS: 492.0 (APCI)+; 490.1 (APCI)-; HPLC (method A): >99% purity; t_R = 12.32 min. Anal. Calcd for $C_{30}H_{33}N_7 \cdot 0.09\ CH_2Cl_2$: C, 72.39; H, 6.70; N, 19.64. Found: C, 72.51; H, 6.37; N, 19.27.

*Synthesis of (S)-3-(5-(2-(1H-Tetrazol-5-yl)phenyl)-2,3-dihydro-1H-inden-1-yl)-2-ethyl-7-isobutyl-5-methyl-3H-imidazo[4,5-b]pyridine (**2n**). Step 1. (S)-2-Ethyl-7-isobutyl-5-methyl-3-(5-(2-(1-trityl-1H-tetrazol-5-yl)phenyl)-2,3-dihydro-1H-inden-1-yl)-3H-imidazo[4,5-b]pyridine (**11n**).* Prepared from the approximately 86:14 mixture of 2-ethyl-5-isobutyl-7-methyl-3*H*-imidazo[4,5-*b*]pyridine (**6l**) and 2-ethyl-7-isobutyl-5-methyl-3*H*-imidazo[4,5-*b*]pyridine (**6n**) (2.5 g, 12 mmol) following general procedure **D**. Mixture purified by MPLC to give a mixture of **11l** and **11n** (1.94 g) that was taken directly to the next step without further characterization.

*Step 2. (S)-3-(5-(2-(1H-Tetrazol-5-yl)phenyl)-2,3-dihydro-1H-inden-1-yl)-2-ethyl-7-isobutyl-5-methyl-3H-imidazo[4,5-b]pyridine (**2n**).* Prepared from the mixture of trityl-protected tetrazole **11l** and **11n** (1.3 g, 1.8 mmol) following general procedure **E**. Tetrazole **2n** was obtained as a white solid (45 mg, 5% yield): ^{1}H NMR (DMSO-d_6, 400 MHz) δ 7.64−7.58 (m, 2 H), 7.53−7.49 (m, 2 H), 7.09 (s, 1 H), 6.80 (s, 1 H), 6.73 (d, J = 7.8 Hz, 1 H), 6.67 (d, J = 8.05 Hz, 1 H), 6.31 (bs, 1 H), 3.18−3.15 (m, 1 H), 2.98−2.90 (m, 1 H), 2.69 (d, J = 7.3 Hz, 2 H), 2.63−2.61 (m, 2 H), 2.43 (s, 3 H), 2.18−2.07 (m, 1 H), 1.15 (t, J = 7.3 Hz, 3 H), 0.84 (d, J = 6.6 Hz, 6 H); CIMS: 478.2 (APCI)+; 476.3 (APCI)-; HPLC (method A): 96.12% purity; t_R = 11.79 min.

*Synthesis of (S)-3-(5-(2-(1H-Tetrazol-5-yl)phenyl)-2,3-dihydro-1H-inden-1-yl)-5-benzyl-2-ethyl-7-methyl-3H-imidazo[4,5-b]pyridine (**2o**). Step 1. 2-Amino-6-benzyl-4-methylnicotinamide (**4o**).* Prepared from 2-amidino-acetamide hydrochloride (3.20 g, 23.3 mmol) and 1-phenylpentane-2,4-dione (4.20 g, 23.3 mmol) following general procedure **A**. An approximate 60:40 mixture of 2-amino-6-benzyl-4-methylnicotinamide (**4o**) and 2-amino-4-benzyl-6-methylnicotinamide was obtained (2.44 g, 43%): ^{1}H NMR (400 MHz, DMSO-d_6) δ 2.14, 2.16 (s, 3 h), 3.79, 3.86 (s, 2 H), 5.60, 5.67 (s, 1 H), 6.16, 6.32 (s, 1 H), 7.13−7.31 (m, 5 H), 7.50, 7.56 (bs, 1 H), 7.67, 7.85 (bs, 1 H); CIMS: 242.1 (APCI)+, 240.0 (APCI)-.

*Step 2. 5-Benzyl-7-methyl-1H-imidazo[4,5-b]pyridin-2(3H)-one (**5o**).* Prepared from the mixture of 2-amino-6-benzyl-4-methylnicotinamide (**4o**) and 2-amino-4-benzyl-6-methylnicotinamide (1.80 g, 7.46 mmol) following general procedure **B**. An approximate 3:2 mixture of 5-benzyl-7-methyl-1*H*-imidazo[4,5-*b*]pyridin-2(3*H*)-one (**5o**) and 7-benzyl-5-methyl-1*H*-imidazo[4,5-*b*]pyridin-2(3*H*)-one was obtained (1.62 g, 91% yield): ^{1}H NMR (400 MHz, DMSO-d_6) δ 2.22, 2.29 (s, 3 H), 3.92, 3.93 (s, 2 H), 6.60, 6.68 (s, 1 H), 7.12−7.32 (m, 5 H), 11.11 (bs, 2 H); CIMS: 240.0 (APCI)+, 238.0 (APCI)-.

*Step 3. 5-Benzyl-2-ethyl-7-methyl-3H-imidazo[4,5-b]pyridine (**6o**).* Prepared from the mixture of 5-benzyl-7-methyl-1*H*-imidazo[4,5-*b*]-pyridin-2(3*H*)-one (**5o**) and 7-benzyl-5-methyl-1*H*-imidazo[4,5-*b*]pyridin-2(3*H*)-one (1.50 g, 6.27 mmol), propionic acid (2.81 mL, 37.61 mmol), and propionic anhydride (4.85 mL, 37.61 mmol) following general procedure **C**. An approximate 3:2 mixture of 5-benzyl-2-ethyl-7-methyl-3*H*-imidazo[4,5-*b*]pyridine (**6o**) and 7-benzyl-2-ethyl-5-methyl-3*H*-imidazo[4,5-*b*]pyridine was obtained (1.07 g, 68% yield): ^{1}H NMR (400 MHz, DMSO-d_6) δ 1.26−1.36 (m, 3 H), 2.45, 2.43 (s, 3 H), 2.74−2.89 (m, 2 H), 3.92, 4.05, 4.15, 4.20 (s, 2 H), 6.78, 6.87, 6.90 (s, 1 H), 7.13−7.21 (m, 1 H), 7.22−7.35 (m, 4 H); CIMS: 252.1 (APCI)+, 250.1 (APCI)-.

*Step 4. (S)-5-Benzyl-3-(5-bromo-2,3-dihydro-1H-inden-1-yl)-2-ethyl-7-methyl-3H-imidazo[4,5-b]pyridine (**8o**).* Prepared from the mixture of 5-benzyl-2-ethyl-7-methyl-3*H*-imidazo[4,5-*b*]pyridine (**6o**) and 7-benzyl-2-ethyl-5-methyl-3*H*-imidazo[4,5-*b*]pyridine (1.06 g, 4.22 mmol) following general procedure **F** to provide **8o** as a white solid (1.06 g, 56% yield): ^{1}H NMR (400 MHz, DMSO-d_6) δ 7.60 (d, J = 1.7 Hz, 1 H), 7.26 (dd, J = 7.9, 1.8 Hz, 1 H), 7.08−7.21 (m, 3 H), 7.04 (d, J = 7.1 Hz, 2 H), 6.89 (s, 1 H), 6.76 (d, J = 8 Hz, 1 H), 6.19 (t, J = 8.2 Hz, 1 H), 3.88 (s, 2 H), 3.00−3.13 (m, 1 H), 2.72−3.00 (m, 2 H), 2.54−2.73 (m, 2 H), 2.44 (s, 3 H), 1.31 (t, J = 7.6 Hz, 3 H); CIMS: 448.1 (APCI)+.

*Step 5. (S)-5-Benzyl-2-ethyl-7-methyl-3-(5-(2-(1-trityl-1H-tetrazol-5-yl)phenyl)-2,3-dihydro-1H-inden-1-yl)-3H-imidazo[4,5-b]pyridine (**11o**).* Prepared from bromide **8o** (0.600 g, 1.34 mmol) following general procedure **G** to provide **11o** as a foam (0.479 g, 47% yield): CIMS: 754.3 (APCI)+, 510.2 (APCI)-. Product was taken to the next step without further characterization.

*Step 6. (S)-3-(5-(2-(1H-Tetrazol-5-yl)phenyl)-2,3-dihydro-1H-inden-1-yl)-5-benzyl-2-ethyl-7-methyl-3H-imidazo[4,5-b]pyridine (**2o**).* Prepared from trityl-protected tetrazole **11o** (0.479 g, 0.635 mmol) following general procedure **E** to afford **2o** as a pale yellow solid (0.146 g, 45%): ^{1}H NMR (400 MHz, DMSO-d_6) δ 7.62−7.74 (m, 2 H), 7.51−7.62 (m, 2 H), 7.06−7.21 (m, 6 H), 6.89 (s, 1 H),

6.70−6.82 (m, 2 H), 6.30 (bs, 1 H), 3.96 (bs, 2 H), 2.92−3.05 (m, 1 H), 2.82 (bs, 1 H), 2.61−2.73 (m, 2 H), 2.52−2.59 (m, 1 H), 2.45 (s, 3 H), 1.27 (t, J = 7.2 Hz, 3 H); CIMS: 512.2 (APCI)+, 510.2 (APCI)-; HPLC (method A): 98.27% purity; t_R = 11.854 min.

*Synthesis of (S)-2-(1-(2-Ethyl-5-isobutyl-7-methyl-3H-imidazo[4,5-b]pyridin-3-yl)-2,3-dihydro-1H-inden-5-yl)benzoic Acid (**14**). Step 1. (S)-Ethyl 2-(1-(2-ethyl-5-isobutyl-7-methyl-3H-imidazo[4,5-b]pyridin-3-yl)-2,3-dihydro-1H-inden-5-yl)benzoate (**13**).* A solution of **8l** (148 mg, 0.36 mmol), 2-(methoxycarbonyl)phenylboronic acid (78 mg, 0.43 mmol), and 0.36 mL of 2 M Na_2CO_3 in 2 mL dioxane were degassed and then treated with $PdCl_2$(dppf) (26 mg, 0.036 mmol). The mixture was then heated at 85 °C under nitrogen for 18 h. The reaction was then cooled, filtered through a bed of Celite, and concentrated *in vacuo*. Purification by MPLC on silica gel eluting with a gradient of ethyl acetate in heptane (0% to 70%) provided **13** as an off-white solid (78 mg, 46% yield): ^{1}H NMR (400 MHz, $CDCl_3$) δ 7.78 (dd, J = 1.1, 7.7 Hz, 1H), 7.42−7.55 (m, 1H), 7.30−7.41 (m, 2H), 7.26 (s, 1H), 7.03 (d, J = 7.8 Hz, 1H), 6.87 (d, J = 7.8 Hz, 1H), 6.78 (s, 1H), 6.50 (br s, 1H), 3.56−3.65 (m, 3H), 3.25−3.41 (m, 1H), 3.11 (td, J = 8.4, 16.3 Hz, 1H), 2.67−2.89 (m, 2H), 2.43−2.66 (m, 6H), 2.02 (td, J = 6.6, 13 Hz, 1H), 1.31 (t, J = 7.4 Hz, 3H), 0.74−0.93 (m, 6H); CIMS: 468.4 (ESI)+.

*Step 2. (S)-2-(1-(2-Ethyl-5-isobutyl-7-methyl-3H-imidazo[4,5-b]pyridin-3-yl)-2,3-dihydro-1H-inden-5-yl)benzoic Acid (**14**).* A solution of ester **13** (50 mg, 0.11 mmol) in 10 mL methanol was treated with 3 mL 1 M NaOH (3 mmol). The reaction was then heated at 100 °C for 24 h. The reaction was cooled and adjusted to pH 2 with 1 M HCl resulting in the formation of a precipitate. The precipitate was collected by filtration, washed with water, and air-dried to give the title compound (46 mg, 95%) as a beige solid: ^{1}H NMR (400 MHz, $CDCl_3$) δ 7.93 (dd, J = 1.3, 7.7 Hz, 1H), 7.51−7.57 (m, 1H), 7.42 (dt, J = 1.2, 7.6 Hz, 1H), 7.34 (s, 1H), 7.30 (dd, J = 1.2, 7.6 Hz, 1H), 7.13 (d, J = 8.0 Hz, 1H), 7.02 (s, 1H), 6.89 (d, J = 8.0 Hz, 1H), 6.65 (br s, 1H), 3.19 (td, J = 8.3, 16.3 Hz, 2H), 3.00 (br s, 2H), 2.87−3.00 (m, 2H), 2.79 (s, 3H), 2.64 (d, J = 7.0 Hz, 2H), 2.49 (br s, 2H), 1.33−1.44 (m, 3H), 1.22−1.25 (m, 1H), 1.19−1.22 (m, 1H), 0.84 (t, J = 5.8 Hz, 6H); CIMS: 454.4 (ESI)+; HPLC (method A1): 97.29 purity; t_R = 6.954 min.

All PPAR *in vitro* assays and pharmacokinetic study in rat were carried out as previously reported.[33,34]

Characterization of Dissociation Rate of Angiotensin II Receptor Antagonists from the Type 1 Receptor. The radioligand ^{125}I-angiotensin II (^{125}I-Sar^1-Ile^8-Angiotensin II), and human angiotensin II receptor, subtype-1(hAT1) coated Flashplates were both purchased from PerkinElmer Life Sciences (Boston, MA). Test compounds were prepared as 10 μM solutions in binding buffer (50 mM Tris-HCl, pH 7.4, 5 mM $MgCl_2$, 1 mM EDTA, and 0.2% BSA) and incubated in Flashplates at room temperature for 60 min. For nonspecific binding (N) determination, 10 μM of AT II was spiked into the binding buffer during the incubation. After incubation, the plate was washed 3 times with binding buffer and 2 nM of ^{125}I-AT II (3 x K_d) in binding buffer was added to the plate and the radioactivity was counted in TopCount immediately and at regular intervals out to 8 h. As compound dissociated from the receptor, Ang II radioligand was available in excess to bind to the free receptor, so allowing dissociation to be measured as the appearance of counts over time. The percent binding was calculated as $([B - N]/[B_0 - N]) \times 100\%$, where ($B$) is the binding activity in the presence of each compound and (B_0) is in the absence of any drug. The percent inhibition was calculated by subtracting the percent bound from 100. The dissociation curve was generated by plotting percent inhibition against incubation time after radioligand was added. Dissociation rate was calculated in *PRISM* (GraphPad, San Diego, CA) using the formula $Y = 100 \times \exp[-K \times x]$.

Spontaneously Hypertensive Rat Studies. SHR rats arrived from suppliers (SHR/NCrl, Charles River, Wilmington MA) at 12−16 weeks old and allowed 1 week to acclimate. Once acclimated, rats were anesthetized with Telazol (1:1 tiletamine HCl and zolazepam HCl) 20−40 mg/kg IM and the descending aorta exposed via a midline incision. Radiotelemetry transmitters with polyethylene tubing (TA11PA-C40) were inserted into the aorta via an undersize hole below the renal arteries. The cannula was secured in the aorta using a "purse string" suture (6−0 suture) to allow anterograde blood flow to the hindlimb vascular bed. The body of the transmitter was secured on the inside of left abdominal wall and the cannula was anchored to the psoas muscle. The midline incision was closed in two steps using continuous over and over sutures. Each rat was then given penicillin 30 000 units IM, returned to cages, and allowed to recover postoperatively for a minimum of 1 week. During that recovery week, patency and quality of the BP and HR signals from the transmitter were tested to ensure that animals were viable for study inclusion. On the day before the study, blood pressure data were collected and mean average BP over a 2 h period was determined. Rats were subsequently randomized based on BP and allocated to treatment groups to ensure consistency in baseline recordings. On the first day of the study (termed Day 0), all animals received the vehicle treatment via oral gavage and BP was followed for 20 h postdose. On the following day (Day 1), rats received the allocated treatment and again BP was followed for 20 h postdose. Each animal was used as its own control to derive changes in BP by calculating differences between Day 0 and Day 1. All experiments utilizing animals were reviewed and approved by Pfizer's Institutional Animal Care and Use Committee.

In Vivo ZDF Rat Studies. Male Zucker Diabetic Fatty (ZDF/*Lepr*^{fa}- Crl) rats were obtained from Charles River Laboratories (Portage, MI). The ZDF male rat normally presents with NIDDM, transient hyperinsulinemia, and hypertriglyceridemia. Rats were pair housed under a 12 h light/dark cycle with free access to water and Purina 5008 rat chow (protein 26.8%, fat 16.7%, carbohydrates 56.5% kcal/vol; Purina Mills, Richmond, IN). Prior to the onset of diabetic hyperglycemia (approximately 6 weeks of age, fed blood glucose <200 mg/dL), rats were allocated into groups by following a postprandial, conscious tail venipuncture. Tail venipuncture in nonanesthetized, postprandial animals was performed weekly to determine blood glucose, insulin, adiponectin, triglycerides, and free fatty acid measurements. Glucose levels were determined with a HemoCue Glucose Monitor (Ryan Diagnostics), insulin, and adiponectin were determined by ELISA (Alpco), triglycerides were determined by Cobas Mira Analyzer (Roche) and FFA by enzymatic assays (Wako). Rats were administered a once daily oral dose for 7 weeks with suspensions of vehicle alone (1.5% carboxymethyl−cellulose, 0.2% Tween 20), or vehicle plus test compound at the specified dose. All experiments utilizing animals were reviewed and approved by Pfizer's Institutional Animal Care and Use Committee.

X-ray Crystallography. A truncated construct of human PPARγ ligand binding domain (PPARγ-LBD) containing residues Glu207 to Tyr477 was recombinantly expressed in *E. coli*, purified, and crystallized as previously described.[33,34] Crystals were soaked overnight in a 0.8 mM solution of **2a** at room temperature prior to flash-cooling in 25% glycerol. X-ray diffraction data were collected at a wavelength of 1.00 Å at 100 K on the Industrial Macromolecular Crystallographer Association (IMCA) beamline 17-ID at the Advanced Photon Source, Argonne National Laboratories. Diffraction data were processed using Denzo and Scalepack in the HKL2000 program suite.[46] The space group was determined to be centered monoclinic $C2$ with two molecules per asymmetric unit, corresponding to a solvent content of ~50% The structure was determined by the method of Fourier difference using the homodimer of human PPARγ-LBD (3IA6) in the CCP4i suite.[47,48] Structural refinement calculations and electron density maps were calculated with the program Refmac5 in the CCP4i suite or the AutoBuster program using the complete data with no resolution or sigma cutoff.[49,50] Manual fitting and real space refinement of the model

was performed with the program Coot.[51] The final model of PPARγ-LBD consists of two monomers of PPARγ-LBD, 2 molecules of **2a** and 93 water molecules with the refinement statistics, R_{work} = 26.7%, R_{free} = 31.4% (see Supporting Information S-Table 1). The coordinates and structure factors may be found in the Protein Data Bank[47] under the ID codes: 3R8A.pdb and 3R8A.sf.

■ ASSOCIATED CONTENT

Supporting Information. Crystallographic data collection and structure refinement statistics. This material is available free of charge via the Internet at http://pubs.acs.org.

Accession Codes

†Structure deposited in the RCSB Protein Data Bank under PDB ID:3R8A.

■ AUTHOR INFORMATION

Corresponding Author

*(A. C.-G.) Phone: (860) 686-9155. Fax: (860) 686-5256. E-mail: agustin.casimiro-garcia@pfizer.com. (G. F. F.) Phone: (860) 686-3546. E-mail: gary.filzen@pfizer.com.

■ ACKNOWLEDGMENT

Use of the IMCA-CAT beamline 17-ID at the Advanced Photon Source was supported by the companies of the Industrial Macromolecular Crystallography Association through a contract with Illinois Institute of Technology. Use of the Advanced Photon Source was supported by the U.S. Department of Energy, Office of Science, Office of Basic Energy Sciences, under Contract No. W-31-109-Eng-38. Special thanks to Dr. Jack Bikker for technical assistance in rendering Figure 3.

■ ABBREVIATIONS

ACE, angiotensin converting enzyme; ARB, angiotensin receptor blocker; AT1, angiotensin II type 1 receptor; BP, blood pressure; BW, body weight; CV, cardiovascular; DPP-4, dipeptidyl peptidase 4; FFA, free fatty acids; GLP-1, glucagon-like peptide-1; LBD, ligand binding domain; PK, pharmacokinetic; PPARγ, peroxisome proliferator-activated receptor-γ; SFC, supercritical fluid chromatography; SHR, spontaneously hypertensive rat; TG, triglycerides; TZD, thiazolidinedione; ZDF, Zucker diabetic fatty rat

■ REFERENCES

(1) Alberti, K. G. M. M.; Eckel, R. H.; Grundy, S. M.; Zimmet, P. Z.; Cleeman, J. I.; Donato, K. A.; Fruchart, J.-C.; James, W. P. T.; Loria, C. M.; Smith, S. C., Jr. Harmonizing the metabolic syndrome: a joint interim statement of the international diabetes federation task force on epidemiology and prevention; national heart, lung, and blood institute; american heart association; world heart federation; international atherosclerosis society; and international association for the study of obesity. *Circulation* **2009**, *120*, 1640–1645.

(2) Cutler, J. A.; Davis, B. R. Thiazide-type diuretics and beta-adrenergic blockers as first-line drug treatments for hypertension. *Circulation* **2008**, *117*, 2691–2704.

(3) Messerli, F. H.; Beevers, D. G.; Franklin, S. S.; Pickering, T. G. β-Blockers in hypertension-the emperor has no clothes: an open letter to present and prospective drafters of new guidelines for the treatment of hypertension. *Am. J. Hypertens.* **2003**, *16*, 870–873.

(4) Bertrand, M. E. Provision of cardiovascular protection by ACE inhibitors: a review of recent trials. *Curr. Med. Res. Opin.* **2004**, *20*, 1559–1569.

(5) Guazzi, M. D.; Polese, A.; Fiorentini, C.; Bartorelli, A.; Moruzzi, P. Treatment of hypertension with calcium antagonists. *Hypertension* **1983**, *5*, II85–90.

(6) Heran, B. S.; Wong, M. M.; Heran, I. K.; Wright, J. M. Blood pressure lowering efficacy of angiotensin receptor blockers for primary hypertension. *Cochrane Database Syst. Rev.* **2008**, *4*, CD003822.

(7) Moutzouri, E.; Florentin, M.; Elisaf, M. S.; Mikhailidis, D. P.; Liberopoulos, E. N. Aliskiren, a direct renin inhibitor, in clinical practice: a new approach in the treatment of hypertension. *Curr. Vasc. Pharmacol.* **2010**, *8*, 344–362.

(8) Lloyd-Jones, D.; Adams, R.; Carnethon, M.; De Simone, G.; Ferguson, T. B.; Flegal, K.; Ford, E.; Furie, K.; Go, A.; Greenlund, K.; Haase, N.; Hailpern, S.; Ho, M.; Howard, V. The american heart association statistics committee and stroke statistics subcommittee. *Circulation* **2009**, *119*, e21–e181.

(9) Saydah, S. H.; Eberhardt, M. S.; Loria, C. M.; Brancati, F. L. Subclinical stales of glucose intolerance and risk of death in the US. *Diabetes Care* **2001**, *24*, 447–453.

(10) Khaw, K. T.; Wareham, N.; Bingham, S.; Luben, R.; Welch, A.; Day, N. Association of hemoglobin A1c with cardiovascular disease and mortality in adults: the European prospective investigation into cancer in Norfolk. *Ann. Intern. Med.* **2004**, *141*, 413–420.

(11) Klein, S.; Sheard, N. F.; Pi-Sunyer, X.; Daly, A.; Wylie-Rosett, J.; Kulkarni, K.; Clark, N. G. Weight management through lifestyle modification for the prevention and management of type 2 diabetes: rationale and strategies: a statement of the American Diabetes Association, the North American Association for the Study of Obesity, and the American Society for Clinical Nutrition. *Diabetes Care* **2004**, *27*, 2067–2073.

(12) Chia, C. W.; Egan, J. M. Role and development of GLP-1 receptor agonists in the management of diabetes. *Diabetes Metab. Syndr. Obes.* **2009**, *2*, 37–49.

(13) Drab, S. R. Incretin-based therapies for type 2 diabetes mellitus: current status and future prospects. *Pharmacotherapy* **2010**, *30*, 609–624.

(14) Choi, J. H.; Banks, A. S.; Estall, J. L.; Kajimura, S.; Bostrom, P.; Laznik, D.; Ruas, J. L.; Chalmers, M. J.; Kamenecka, T. M.; Bluher, M.; Griffin, P. R.; Spiegelman, B. M. Anti-diabetic drugs inhibit obesity-linked phosphorylation of PPARγ by Cdk5. *Nature* **2010**, *466*, 451.

(15) de Gasparo, M.; Catt, K. J.; Inagami, T.; Wright, J. W.; Unger, T. International union of pharmacology. XXIII. The angiotensin II receptors. *Pharmacol. Rev.* **2000**, *52*, 415–472.

(16) Benson, S. C.; Pershadsingh, H. A.; Ho, C. I.; Chittiboyina, A.; Desai, P.; Pravenec, M.; Qi, N.; Wang, J.; Avery, M. A.; Kurtz, T. W. Identification of telmisartan as a unique angiotensin II receptor antagonist with selective PPARγ-modulating activity. *Hypertension* **2004**, *43*, 993–1002.

(17) Vitale, C.; Mercuro, G.; Castiglioni, C.; Cornoldi, A.; Tulli, A.; Fini, M.; Volterrani, M.; Rosano, G. M. C. Metabolic effect of telmisartan and losartan in hypertensive patients with metabolic syndrome. *Cardiovasc. Diabetol.* **2005**, *4*, 6–13.

(18) Goebel, M.; Clemenz, M.; Staels, B.; Unger, T.; Kintscher, U.; Gust, R. Characterization of new PPARγ agonists: analysis of telmisartan's structural components. *ChemMedChem* **2009**, *4*, 445–456.

(19) Goebel, M.; Staels, B.; Unger, T.; Kintscher, U.; Gust, R. Characterization of New PPARγ Agonists: Benzimidazole Derivatives - the Importance of Position 2. *ChemMedChem* **2009**, *4*, 1136–1142.

(20) Goebel, M.; Wolber, G.; Markt, P.; Staels, B.; Unger, T.; Kintscher, U.; Gust, R. Characterization of new PPARγ agonists: Benzimidazole derivatives-importance of positions 5 and 6, and computational studies on the binding mode. *Bioorg. Med. Chem.* **2010**, *18*, 5885–5895.

(21) Chittiboyina, A. G.; Mizuno, C. S.; Desai, P. V.; Patny, A.; Kurtz, T. W.; Pershadsingh, H. A.; Speth, R. C.; Karamyan, V.; Avery, M. A. Design, synthesis, and docking studies of novel telmisartan-glitazone hybrid analogs for the treatment of metabolic syndrome. *Med. Chem. Res.* **2009**, *18*, 589–610.

(22) Mizuno, C. S.; Chittiboyina, A. G.; Patny, A.; Kurtz, T. W.; Pershadsingh, H. A.; Speth, R. C.; Karamyan, V. T.; Avery, M. A. Design, synthesis, and docking studies of telmisartan analogs for the treatment of metabolic syndrome. *Med. Chem. Res.* **2009**, *18*, 611–628.

(23) Mizuno, C. S.; Chittiboyina, A. G.; Shah, F. H.; Patny, A.; Kurtz, T. W.; Pershadsingh, H. A.; Speth, R. C.; Karamyan, V. T.; Carvalho, P. B.; Avery, M. A. Design, Synthesis, and Docking Studies of Novel Benzimidazoles for the Treatment of Metabolic Syndrome. *J. Med. Chem.* **2010**, *53*, 1076–1085.

(24) A preliminary report of this work was presented recently: Casimiro-Garcia, A.; Bigge, C. F.; Chen, J.; Davis, J. A.; Dudley, D. A.; Edmunds, J. J.; Esmaeil, N.; Filzen, G.; Flynn, D.; Geyer, A.; Heemstra, R. J.; Jalaie, M.; Ohren, J. F.; Padalino, T.; Pulaski, J.; Schaum, R. P.; Stoner, C. L. Discovery of a series of imidazo[4,5-*b*]pyridines with dual action as angiotensin II type 1 receptor (AT1) antagonists and partial PPARgamma agonists. 239th American Chemical Society Meeting, San Francisco, CA, United States. March 2010. MEDI-200.

(25) Carpino, P. A.; Wester, R. T.; Da Silva Jardine, P. A. Angiotensin II receptor antagonists. US5338740. 1994.

(26) Carpino, P. A.; Sneddon, S. F.; Da Silva Jardine, P.; Magnus-Ayritey, G. T.; Rauch, A. L.; Burkard, M. R. A conformationally restrained series of AT1-selective angiotensin II antagonists. *Bioorg. Med. Chem. Lett.* **1994**, *4*, 93–98.

(27) Senanayake, C. H.; Fredenburgh, L. E.; Reamer, R. A.; Liu, J.; Larsen, R. D.; Verhoeven, T. R.; Reider, P. J. Magnesium-assisted imidazole formation from unreactive ureas. *Tetrahedron Lett.* **1994**, *35*, 5775–5778.

(28) Corey, E. J.; Bakshi, R. K.; Shibata, S. Highly enantioselective borane reduction of ketones catalyzed by chiral oxazaborolidines. Mechanism and synthetic implications. *J. Am. Chem. Soc.* **1987**, *109*, 5551–5553.

(29) Corey, E. J.; Helal, C. J. Reduction of carbonyl compounds with chiral oxazaborolidine catalysts: A new paradigm for enantioselective catalysis and a powerful new synthetic method. *Angew. Chem., Int. Ed.* **1998**, *37*, 1986–2012.

(30) Lo, Y. S.; Rossano, L. T. Preparation of tetrazolylphenylboronic acid intermediates for the synthesis of angiotensin II receptor antagonists. US5130439. 1992.

(31) Mantlo, N. B.; Chakravarty, P. K.; Ondeyka, D. L.; Siegl, P. K. S.; Chang, R. S.; Lotti, V. J.; Faust, K. A.; Schorn, T. W.; Chen, T. B.; Schorn, T. W.; Sweet, C. S.; Emmert, S. E.; A., P. A.; J., G. W. Potent, orally active imidazo[4,5-*b*]pyridine-based angiotensin II receptor antagonists. *J. Med. Chem.* **1991**, *34*, 2919–2922.

(32) Hulin, B.; Clark, D. A.; Goldstein, S. W.; McDermott, R. E.; Dambek, P. J.; Kappeler, W. H.; Lamphere, C. H.; Lewis, D. M.; Rizzi, J. P. Novel thiazolidine-2,4-diones as potent euglycemic agents. *J. Med. Chem.* **1992**, *35*, 1853–1864.

(33) Casimiro-Garcia, A.; Bigge, C. F.; Davis, J. A.; Padalino, T.; Pulaski, J.; Ohren, J. F.; McConnell, P.; Kane, C. D.; Royer, L. J.; Stevens, K. A.; Auerbach, B. J.; Collard, W. T.; McGregor, C.; Fakhoury, S. A.; Schaum, R. P.; Zhou, H. Effects of modifications of the linker in a series of phenylpropanoic acid derivatives: Synthesis, evaluation as PPARα/γ dual agonists, and X-ray crystallographic studies. *Bioorg. Med. Chem.* **2008**, *16*, 4883–4907.

(34) Casimiro-Garcia, A.; Bigge, C. F.; Davis, J. A.; Padalino, T.; Pulaski, J.; Ohren, J. F.; McConnell, P.; Kane, C. D.; Royer, L. J.; Stevens, K. A.; Auerbach, B.; Collard, W.; McGregor, C.; Song, K. Synthesis and evaluation of novel α-heteroaryl-phenylpropanoic acid derivatives as PPARα/γ dual agonists. *Bioorg. Med. Chem.* **2009**, *17*, 7113–7125.

(35) Xu, H. E.; Lambert, M. H.; Montana, V. G.; Plunket, K. D.; Moore, L. B.; Collins, J. L.; Oplinger, J. A.; Kliewer, S. A.; Gampe, R. T., Jr.; McKee, D. D.; Moore, J. T.; Willson, T. M. Structural determinants of ligand binding selectivity between the peroxisome proliferator-activated receptors. *Proc. Natl. Acad. Sci. U.S.A.* **2001**, *98*, 13919–13924.

(36) Nettles, K. W. Insights into PPARγ from structures with endogenous and covalently bound ligands. *Nat. Struct. Mol. Biol.* **2008**, *15*, 893–895.

(37) Nolte, R. T.; Wisely, G. B.; Westin, S.; Cobb, J. E.; Lambert, M. H.; Kurokawa, R.; Rosenfeld, M. G.; Willson, T. M.; Glass, C. K.; Milburn, M. V. Ligand binding and co-activator assembly of the peroxisome proliferator-activated receptor-γ. *Nature* **1998**, *395*, 137–143.

(38) Patani, G. A.; LaVoie, E. J. Bioisosterism: a rational approach in drug design. *Chem. Rev.* **1996**, *96*, 3147–3176.

(39) Middlemiss, D.; Watson, S. P. A medicinal chemistry case study. An account of an angiotensin II antagonist drug discovery programme. *Tetrahedron* **1994**, *50*, 13049–13080.

(40) Wexler, R. R.; Greenlee, W. J.; Irvin, J. D.; Goldberg, M. R.; Prendergast, K.; Smith, R. D.; Timmermans, P. B. M. W. M Nonpeptide angiotensin II receptor antagonists: the next generation in antihypertensive therapy. *J. Med. Chem.* **1996**, *39*, 625–656.

(41) Morsing, P.; Adler, G.; Brandt-Eliasson, U.; Karp, L.; Ohlson, K.; Renberg, L.; Sjoquist, P.-O.; Abrahamsson, T. Mechanistic differences of various AT1-receptor blockers in isolated vessels of different origin. *Hypertension* **1999**, *33*, 1406–1413.

(42) Gradman, A. H. AT1-receptor blockers: differences that matter. *J. Hum. Hypertens.* **2002**, *16*, S9–S16.

(43) Maillard, M. P.; Perregaux, C.; Centeno, C.; Stangier, J.; Wienen, W.; Brunner, H.-R.; Burnier, M. In vitro and in vivo characterization of the activity of telmisartan: an insurmountable angiotensin II receptor antagonist. *J. Pharmacol. Exp. Ther.* **2002**, *302*, 1089–1095.

(44) Sharpe, M.; Jarvis, B.; Goa, K. L. Telmisartan: a review of its use in hypertension. *Drugs* **2001**, *61*, 1501–1529.

(45) Stucky, G.; Imwinkelried, R. Preparation of imidazopyridines. EP645389. 1995.

(46) Otwinowski, Z.; Minor, W. Processing of x-ray diffraction data collected in oscillation mode. In *Macromolecular Crystallography, Part A.*, Carter, C. W., Jr.; Sweet, R. M., Ed. Academic Press: New York, 1997; Vol. 276, pp 307−326.

(47) Berman, H. M.; Westbrook, J.; Feng, Z.; Gilliland, G.; Bhat, T. N.; Weissig, H.; Shindyalov, I. N.; Bourne, P. E. The Protein Data Bank. *Nucleic Acids Res.* **2000**, *28*, 235–242.

(48) Bailey, S. The CCP4 suite: programs for protein crystallography. *Acta Crystallogr.* **1994**, *D50*, 760–763.

(49) Murshudov, G. N.; Vagin, A. A.; Dodson, E. J. Refinement of macromolecular structures by the maximum-likelihood method. *Acta Crystallogr.* **1997**, *D53*, 240–255.

(50) Roversi, P.; Blanc, E.; Vonrhein, C.; Evans, G.; Bricogne, G. Modelling prior distributions of atoms for macromolecular refinement and completion. *Acta Crystallogr.* **2000**, *D56*, 1316–1323.

(51) Emsley, P.; Lohkamp, B.; Scott, W. G.; Cowtan, K. Features and development of Coot. *Acta Crystallogr.* **2010**, *D66*, 486–501.